POLITECNICO DI TORINO

Master Degree in Biomedical Engineering

The memory of fluids: an exploratory study for the geometrical description of a fluidic channel using the Shannon's information Theory

Supervisor
Prof. Umberto Morbiducci
Co-supervisor
Ph.D. Simone Ripandelli

Candidate
Marta Sotgiu

July 2018

Ai miei genitori,

grazie per aver sempre creduto in me.

<< In the middle of every difficulty lies opportunity >>

A. Einstein

Dopo questi anni di sacrifici e sofferenze ma anche gioie e soddisfazioni, ritengo indispensabile e doveroso ringraziare tutte le persone che, in un modo o nell'altro, mi hanno permesso di crescere, di farmi credere in me stessa e che non mi hanno mai fatto mancare il loro indispensabile supporto. Arrivata ormai alla fine di questo percorso, mi sento di dire un grazie sincero in particolar modo ad alcune persone:

Al prof. Morbiducci, per l'opportunità che mi ha concesso in questo lungo anno che mi ha permesso di crescere didatticamente ma soprattutto come persona.
A Simone, perché senza il suo enorme aiuto questo lavoro non avrebbe mai preso forma. Grazie per avermi fatto capire che la pazienza e l'impegno portano sempre a dei risultati.

Alla mia famiglia, un grazie immenso ai miei fratelli, ai miei zii e a chi è sempre stato con me. Soprattutto voi, mamma e babbo, che in questi anni non avete mai smesso di starmi accanto, di supportarmi e di rimproverarmi quando era necessario. Non potrò mai rendere giustizia a ciò che avete fatto e che sempre farete per me. Nel mio piccolo spero di avervi oggi reso orgogliosi di me.

Alla mia "famiglia" torinese, i San Bodri… senza i quali questi anni non sarebbero stati così belli. Non è necessario citarvi uno ad uno ma voi sapete. Grazie per la spensieratezza, l'appoggio, le risate e le innumerevoli serate passate insieme, anche nelle difficoltà. Un particolare grazie è doveroso ai miei primi due compagni di avventura: Gianlu, per avermi subito accolta come se ci conoscessimo da sempre e Richi, una spalla su cui so di poter sempre contare. Grazie per esserti sempre fatto in quattro quando avevo bisogno. Casa Piras sarà sempre nel mio cuore.

A tutti miei amici sardi che nei miei rientri a casa mi hanno sempre fatto pensare che niente fosse cambiato. Grazie in particolare alle amiche di sempre che nonostante la lontananza non mi hanno mai fatto mancare l'appoggio e il supporto.

A tutti gli amici della sala tesisti per questi mesi insieme. Non posso non dire grazie soprattutto a Michela e Katia che sono state le due colonne di questo anno al Poli, ci siete sempre state e non avete idea di quanto mi abbiate aiutata, per questo vi ringrazierò sempre.

Un grazie che non può essere quantificato va a te, Lore, non basterebbero mille parole per renderti onore. Senza di te questo giorno non sarebbe mai arrivato e, con tutte le sofferenze passate insieme, in parte la mia laurea è anche tua. Grazie per non essere mai mancato, per esserci stato sia nei momenti peggiori che in quelli migliori e per non aver mai dubitato di me, dandomi la forza di continuare fino ad oggi. Grazie, senza di te non ce l'avrei mai fatta.

Abstract

Does a fluid have memory? Is it possible to interrogate it about the information it is carrying while it flows?

These questions come observing the Nature and the ability of many natural systems to store information. This capability is common for many materials solid or semi-solid. An example can be found into the geology field where, through the study of subsoil's stratigraphy, surfaces that move relatively in relation to each another are investigated. The information in this case is in the mineral that is at the interface between the two surfaces. Under the friction's effect, that produces energy in the form of heat, the structure of the mineral change. The solid material behaves like an extremely high-density fluid under the effect of tectonic movements, deforming itself to create undulating layers that give the idea that the rock has been bent. When something happens, it is recorded into the material itself. In nature there are also situations where fluids "survive" in a state where the transformations take a long time to end. It happens in many biological systems as the human cardiovascular system that can be considered a great micro-fluidic one. These are just examples, but the list can be longer. The idea is simple: an open system that is able to interact with the environment that surrounds itself, is even able to receive an information during this interaction under different forms; energy or matter. Under these considerations this research has been developed. The aim of the study, indeed, was to investigate the fluid systems in order to understand, under defined conditions, its capability to store information on time when it flows in a channel (and also the limits of this capability).

Since a fluid is moving means that it has the energy to do it. It follows that the fluid system during the flow modifies its internal energy generating a variation of Entropy of the system, in a purely thermodynamic meaning. It is common to study fluidic systems by a mechanical point of view, while in this research the idea is to approach the study from another point of view, applying an energetic analysis (thermodynamic) focusing on the entropy itself.

The own definition of entropy is not totally univocal, but can be explained as the level of disorder of a system and especially describes its evolution under the effect of the external environment. From this interpretation, the concept of entropy was taken up by Claude Shannon in 1948 [1] when he applied the concept in the field of information theory, in order to describe the level of complexity of a signal in data communication system: the thermodynamic of the information. Even a fluid, from a certain point of view, is a way to bring the information. The nature uses it to transport nutrients to cells (biology) and in the same systems to transport “information”. In more complex biological systems like human body, in case of inflammations, the blood is on charge to communicate the situation with the central nervous system. For these reasons, a parallelism with a fluid that flows in a micro-fluidic channel will be proposed in this study, considering the transmitter the inlet of the channel and the receiver the outlet of the channel. The fluid that flows in the channel has been considered as a carrier and, consequently, as a reservoir of information related to the environment. In the event of presence of obstacles in the channel, the fluid adapts itself to the geometry during motion, so the particles change their trajectories. This variation can be casual (i.e. in presence of turbulence) or, under specific constraints and boundary conditions, not. This behaviour influences the internal energy of the system and consequently the entropy. It follows that entropy could have all the characteristics to be a descriptor of the state of a system when its configuration changes.

Therefore, another aim of the study is to find a relation between the interaction of the fluid and the shape of the obstacles present into the channel through the Shannon entropy parameter. To achieve this goal, a Computational Fluid Dynamic (CFD) simulation using the software ANSYS FLUENT® v.15.0 was made, where a 2D rectangular channel in presence of obstacles was simulated. In particular, the obstacles have been considered in different shapes, geometries and number in order to evaluate their different impact on the fluid. This analysis was carried out considering initially all the elements of the grid in which the channel was divided and, subsequently, only 50% of the same.

This study can be considered as good starting point to suggest the deepening of this analysis to geometrically describe a channel at the level of presence of obstacles within it. In fact, analysing the parameters linked to entropy, seems to be possible to discriminate their geometry and distribution. Moreover, the analysis of the Shannon entropy considering only 50% of the elements of the grid has provided excellent results. In fact, a very low error rate was obtained compared to the calculation with 100% of the points confirming the validity and solidity of the method.

Contents

List of Figures

List of Tables

Chapter 1

Introduction

During the last years, the study presence of obstacles in a channel or in a vessel has attracted many scientific researchers because of its different applications. As a matter of fact, this situation can be attributes to different and generics scenarios. Obstacles can be seen in different way depending on the field of investigation. For example, in the field of medicine plaques can be seen as obstacles in the blood vessels. Instead, in biology field, this role can be played by the cells that in a bioreactor are used to promote their growth and/or differentiation. In microfluidic field, micro- and nano-reactors can be necessary to operate a fluid mixing and the presence and the amount of the obstacles influence the fluid mixing that, in general, must be monitored.

So, in literature it is common to find several studies that investigate the presence of obstacles in different situations. This phenomenon has particular relevance to numerous practical engineering applications, due to the associated influence of the pressure loss, heat and mass transfer.

In 2015 Chatti *et al.* [2] studied the effect of presence of obstacles in a porous channel from the point of view of the heat transfer, in order to see how these particles could influence the fluid and so the heat transmission. Others similar studies, that were focused on the heat transfer rate in presence of obstacle, were carried out by Gareh

(2014) [3], Bilen and Yapici (2001) [4], Y. Wang and K. Vafai (1999) [5] and Hosseini *et al.* (2008) [6].

Another study about the effect of obstacles in a porous medium has been investigated in 2014 by S.J. Cox [7]. He analysed how much obstacles induced a bubble division in the flow of a foam, uncovering that the position and the size of the obstacles had a bearing in the bubble division. Sure enough, they could produce either only lower changes or significant number of division events and so the foams were highly poly-dispersed.

The presence of obstacles is also investigated for the acoustic oscillations of a gas in a channel. In his paper, in 2011, Khasanov [8], discussed about the reliance of the self-oscillation frequencies on the size of the obstacle. He focused his attention to demonstrate the dependences of the frequencies of eigenoscillations on the obstacle lengths and locations along the channel.

Moreover, in literature there are different fluid dynamic studies in which is treated the phenomenon of the obstacle presence, and many of them are focused in particular for biomedical micro-devices.

Merdasi *et al.* (2017) [9] carried out a numerical simulation of a falling droplet subject to gravitational force in a channel with embedded rectangular obstacles. Their aim was to combine effect of the obstacles and fluid parameters to control deformation rate of a falling droplet.

Instead, Yojina *et al.* in 2010 [10] investigated the flow pattern phenomena and the flow field around one and two square obstacles inside a two-dimensional channel for a range of Reynolds (Re) numbers. Their idea was born thanks to the interest for chemical mixing fluidic devices, especially to improving the efficacy of the mixing, hypothesizing that it could be possible through the presence of obstacles along the channel.

A biomedical study was carried out by Bulusu and Plesniak in 2015 [11] with the aim to introduce an autonomous method for the identification of hemodynamic secondary flows. They presented an algorithmic approach using the tenets of the classical theory of communication, Shannon entropy and signal uncertainty, that permit to avoid the human dependence in the research of secondary flows. This “spiral blood flow structures” are ubiquitous in the cardiovascular systems. The authors investigated a stent implantation because, in case of breakdown, it concerns the progression of several cardiovascular diseases due to the alteration of stress distributions near the wall. The observation was made possible using the Shannon entropy-based wavelet transform method for spiral blood flow structures.

Resuming, there are a lot of fields in which the importance of obstacles presence in a channel is studied and, in all of these field, the presence on them plays relevant and different roles.

There is also another key concept that must be underlined and explained for this research: the possible influence that an object may have in terms of “induced” information or that can reside in an entity (i.e. an obstacle is an entity) when it is undergo a transformation. The idea is that there are several cases in which an open system is able to accept information from the environment that surround it, cause of their interaction. One of the most important hypotheses for this study is related to the fact that a system always evolves in different ways according to the boundary conditions. Moreover, each evolving system possesses a certain digital imprint that characterizes it from all the others. Learning how to read this imprint allows to get to the complete knowledge of the system.

An example of the ability of a material to store information from the surrounding environment can be found in the field of geology. As a matter of fact, geologists are able to observe surfaces that move relatively to each other. In these cases, the information is located in the mineral that is at the interface between the two surfaces. Under the effect of friction that generates energy in the form of heat, it changes the structure of the mineral. When something happens, in a certain way it is recorded into the material itself.

A question arises from these considerations: can a fluid be investigated starting from the information it is carrying while it flows? In this way we are assuming valid the concept that a generic fluid (as it happens for many other materials) has the capacity to absorb (or store) information and then maintain it over time. How long is the capacity to maintain the information is linked to the nature of the fluid itself. However, it must be remembered that fluids undergo very rapid transformations and the information can be lost in such a short period of time that a large part of this, if not all, is lost during motion. On the other hand, in nature there are also situations where fluids "survive" in a state where the transformations take a long time to end. It happens in many biological systems as the human cardiovascular system that can be considered a great micro-fluidic one. So, a fluid, from a certain point of view, is a way to bring the information. The nature uses it to transport nutrients to cells (biology) and in the same systems to transport “information” in more complex system like human body, in case of inflammations, for example.

Therefore, the two starting points for this study were the relevance of obstacles in a channel, and the possibility that a fluid can carry and keep information during its motion.

There are different ways to investigate these situations and, how seen in Bulusu and Plesniak study [11], one of this is the approach employing the entropy theories.

When a fluid is in motion with respect to a system, it means that it has energy to do it. It also signifies that a fluid system in the act of moving modifies its internal energy, lost during motion, also generating a variation of the entropy of the system, in a purely thermodynamic sense (Chapter 2). As a matter of fact, entropy has all the characteristics to be a descriptor of the state of a system when it modifies its configuration. The definition of entropy is not totally univocal, but can be explained as the level of disorder of a system and above all it describes an evolution of the latter, which is transformed under the effect of the external environment that surrounds it. From this interpretation, the concept of entropy was taken up by Shannon [1] in 1948. He applied the concept in the field of information theory, in order to describe the level of complexity of a signal in data communication system: the thermodynamic of the information.

In this study the system was analysed in order to try to extrapolate information about its transformation, passing from the calculation of entropy, but not in the thermodynamic sense, rather from an informative point of view through the concept of entropy of Shannon (better explained in the next chapters).

Information entropy was already used in the past to describe different problems, e.g. a state of disorder in a system and to quantify flow complexity and so also fluid mixing. The first was analysed by Brandani et al. in 2013 [12] through the Shannon and conditional entropy. Instead, in a previous work, in 2006, Camesasca *et al*. [13] quantified fluid mixing with the Shannon entropy. In 2017, Pozo *et al.* [14] applied the study of information entropy introducing an index of flow complexity coined interlacing complexity index (ICI), valid for a single-phase flow in an open system with inlet and outlet regions, involving finite times. In bioengineering field, in 2008, Rocha *et al.* [15] carried out a research to investigate if the Shannon entropy (SE) was able to determine bone remodelling evolution and maturation events during regeneration of bone defects (usually analysed by a human). The SE can be an objective methods of image texture analysis, to describe the structural changes of new-formed bone, based on the tissue organization or disorganization. It could permit to reduce the bias of the observer in determining the quality of the newly formed tissue.

For what has been said previously, the investigation of obstacles presence and the use of Shannon entropy analysis would seem to be two fields of considerable interest. For this reason, in this study they have been connected to each other.

The present work represents a two-dimensional Computational Fluid Dynamic (CFD) numerical investigation of the motion of a fluid in a rectangular channel, it reproduces a microfluidic channel, containing one or more obstacles of different sizes and shapes and placed in different positions. Another aim of the study is to find a relation between the interaction of the fluid and the shape of the obstacles. The information carrying by a fluid can be seen in different shapes. For example, it can be seen in the way of variation of energy or variations in terms of second order dynamic fluid characteristics as a change of velocity or trajectory. The SE has been applied in order to understand if it is a good descriptor to check the obstacles presence, simply analysing the velocity field in the channel.

The possibility to investigate the internal geometry of a channel without invasive techniques, indeed, could be certainly very interesting in a variety of fields. This method could be useful for both *a priori* and *a posteriori* analysis.

In the chapter 2 firstly, by a historical point of view, the concepts of entropy and information are presented, in order to offer e general overview of the theory. *In secundis* the definition and the derivation of Shannon entropy is introduced. Then, it is show the relationship between Shannon's theory and entropy in thermodynamics, and are pointed out the differences and the similarities.

Later, the applications of Shannon entropy are shown evaluating the fields of use.

In the chapter 3, the first part exposed the different steps to create the 2D model for the Computational Fluid Dynamics (CFD) simulation. The different obstacles configuration in the channel are presented. Instead, the second part consist of an exposition of numerical (used by ANSYS FLUENT®) and analytical solution employed in the model to resolve the equations that govern the fluid dynamics. The third part concerns the explanation of the method used in this work. The principal means was the creation of a binary velocity matrix with which the Shannon entropy was calculated.

The Chapter 4 is a presentation of the results obtained after the post-processing of the numerical outcomes obtained by ANSYS FLUENT®. In the first part the Shannon entropy trends in the different configurations analysed will be show. In this situation, the whole grid elements of the channel have been considered. Instead, in the second part, will be present the results obtained by a valuation of Shannon entropy in the 50% of the grid in order to evaluate if the reduction of the number of elements involves a modification in the information studied through the SE.

Finally, in chapter 5 are reported all the conclusions and all the considerations observable from the results obtained with simulation. In particular, the positive and critical aspects of the analysis are considered and are also analysed future expectations.

Chapter 2

<<We known the past but cannot control it. We control the future but cannot know it.>>

Claude Shannon

Entropy and theory of information entropy

How introduced in chapter 1, the concept of information is not univocal. Before defining the difference and the relationship between entropy and information, it is necessary to resume what “information” is. The word "information" is commonly used, so it is often thought that it means something as “knowledge”, “data” etc. The information represents how confident we are of the probability that something will occur. In other words, information is measured based on the number of resources needed to describe a probable event. Higher is the probability of success of the event, less information needs to be forwarded. The information entropy is defined as the means with which is possible to distinguish and choose from different information, it is the average information quantity generated by a stochastic source of data (i.e. not a deterministic process).

The amount of information necessary to describe a system is closely related to its complexity. There is a strong connection between the amount of information and disorder. Considering the algorithmic complexity as a measure of information, more disordered messages are characterised by more information. The relationship between entropy and disorder is mainly due to Boltzmann [16], even if he did not use the word "disorder". He defined that entropy is as large as the number of microscopic configurations that a system can assume is higher. To better explain this concept, consider the example depicted in figure 2.1.

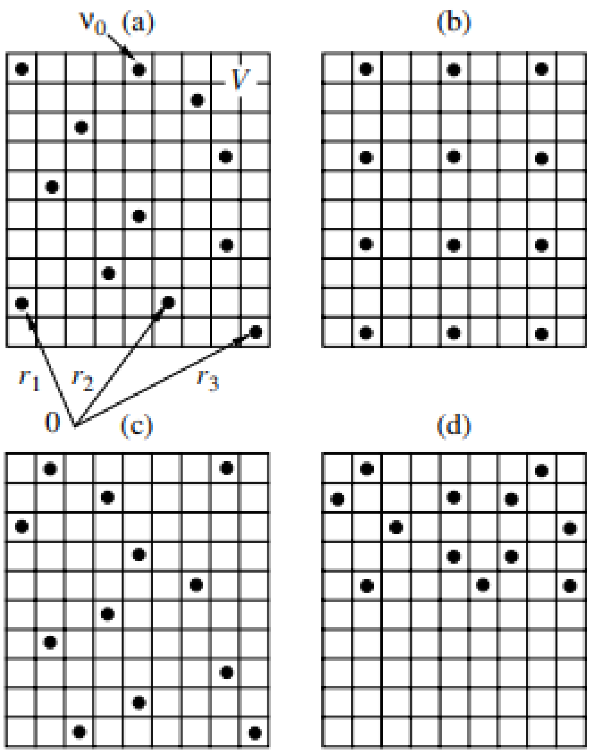

Figure 2.1: Representation of the degree of disorder of a general system: (a, c, d) disordered and (b) crystalline, ordered [17].

The (a), (c) and (d) configurations represented a state with a high disorder while (b) is the ordered state. It follows that the first three are associated to a higher value of entropy due to the large number of configurations that the system can assume compared to the remaining condition.

How is it possible to quantify the average information obtained from knowing an initial message? What are the methods can be used? The answer follows into the next chapters.

2.1 Shannon Entropy

Claude Shannon [1] in 1948 published an article that is considered as a fundamental contribution for the information definition through the theory of information. For the formulation of his theory, Shannon was inspired by Boltzmann, by the formulation of entropy (S).

$$S = \mathrm{k} \log W \tag{2.1}$$

where k is the so called “Boltzmann constant” equal to $1.38054 * 10^{-23}$ J/K.

Shannon observes that a message sent through any type of “channel” is deformed (i.e. a channel is the way with which the message is transmitted or, from another point of view, it is possible to know an event) and therefore some of the information is lost during transmission. He analogized this loss of information with entropy, the well-known function that expresses the degradation of energy that occurs in every transformation of mechanical work into heat.

For Shannon, the starting point was the possibility of misunderstanding and interference during the transmission of a message in a channel, and he asserted that the major role is assumed by the information uncertainly. To make an example and to better explain this concept, you can imagine that tomorrow the sky will be above our head. This is a certain event and it does not surprise us. However, the opposite would surprise us a lot, so a highly unlikely event has a high information value.

In his research, he defined a communication system composed by five principal elements (Figure 2.2):

1. The information source: it is responsible for producing the message.
2. The transmitter: it transforms the message suitable for transmission over the channel.
1. The channel: it is used to transmit the signal from transmitter to receiver.
2. The receiver: it operates a reconstruction of the output message starting from the signal.
3. The destination: the thing for whom the message is intended.

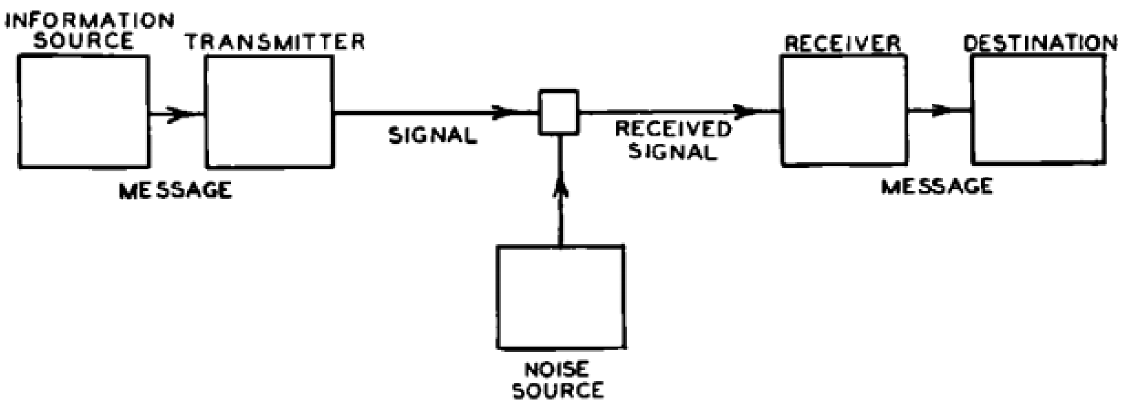

Figure 2.2: Schematic diagram of a general communication system [18]

In his theory, Shannon defined how the information is transferred and therefore the elements necessary for the process. He quantified the minimum number of resources needed to transmit information and named it as "entropy". It is defined in terms of concept of information entropy and now more commonly known as "Shannon entropy". In reality, the idea to employ the noun entropy was not a his one. Myron T. Tribus, an American engineer who became interested in the thermodynamics of information theory, at that time was trying to explain the connection between entropy defined by Claude Shannon and the entropy defined by Rudolf Clausius. In

1961 Tribus met Shannon at MIT (Massachusetts Institute of Technology - Boston) and asked him the reasons for the name “entropy”. In 1971 he claimed that Shannon answered his question thus:

“My greatest concern was what to call it. I thought of calling it ‘information’, but the word was overly used, so I decided to call it ‘uncertainty’. When I discussed it with John von Neumann, he had a better idea. Von Neumann told me, ‘You should call it entropy, for two reasons. In the first place your uncertainty function has been used in statistical mechanics under that name. In the second place, and more importantly, no one knows what entropy really is, so in a debate you will always have the advantage.” (Tribus and McIrving 1971) [19]

For Shannon, the message is selected from a set of possible messages. When one of these is chosen from the set, the information is produced. How said above, there is a minimum number of resources needed to correctly identify the message. In particular, it has to be major or equal to his entropy and a priori knowledge of the data set is fundamental. To better explain this concept, we referred to an example mentioned by Lesne in an article published in 2014. “A classic example is the quantification of the information needed to communicate a play by Shakespeare, whether the receiver knows in advance that he will receive one of the plays by Shakespeare (and then transmitting only the few first words is sufficient), or not (and then the whole text of the play has to be transmitted)” [20].

It is quite common to recognize the Shannon concept of entropy as “binary entropy” because, as minimum units of information, the bits (binary information units) are used. For their definition they can be assume only two values: 0 or 1. In fact, in information theory, two symbols are necessary and sufficient for an alphabet to encode information.

To better explain the concept of entropy, the variables of interest for the study defined in the Shannon theory are presented below.

Supposing to have a set of possible states whose probabilities of occurrence are $X = \{x_i\}_{i=1}^{n}$. The information associated with the i-th event is quantified by:

$$I_p(x_i) = -\log_b P(x_i) \tag{2.2}$$

Where $P(x_i)$ represents the probability of occurrence of the i-th value of x. Shannon introduced the quantity $I_p(x_i)$ as a measure of the information brought by the observation of x, knowing the probability distribution $P(x_i)$. The aim is to find a measure that defines which event will be selected and how much uncertainty affects the result. This measure is now call S and have the following form:

$$S(X) = K \sum_i P(x_i) \cdot I_p(x_i) = -K \sum_i P(x_i) \cdot \log_b P(x_i) \tag{2.3}$$

where K is a positive constant and just depends to a choice of a logarithmic base (b), it corresponds to the choice of a unit for measuring information. It is possible to choose different values for b and this choice reflect to the values of K. How said above, the units chosen are bits, so base 2 is used.

Later in this study the Shannon entropy (SE) will have the following expression:

$$SE(X) = -\sum_i P(x_i) \cdot \log_2 P(x_i) \tag{2.4}$$

In this definition, the convention that $0 \cdot \log_2 0 = 0$ is used, easily justified by continuity since $x \cdot \log x \to 0$ when $x \to 0$.

Information (Eq. 2.2) is strictly related with probability. In fact, it is meaningful only if the message is pull out from a set of messages that could have been issue *a priori*. The receiver assigns to each message a probability before transmission. How explained by Roger Balian in 2004 [21], $I_p(x_i)$ represent so “the surprise in observing x, given prior knowledge on the source summarized in $P(x_i)$”. At this point, it is understandable that the SE symbolize the average missing information, namely, the average information need to point out the outcome when the receiver knows the probability distribution.

For the reasons discussed above, is possible to give another interpretation of the entropy concept, that is, as negative information. Concerning this topic, there were different opinions that were often debated in the past, especially for the concept of negative entropy, discussed i.e. by Léon Brillouin [22] . This consideration derived from the different ideas between Shannon and N.Wiener [23]. In fact, the latter, attributed to entropy the concept of disorganization while the information symbolized organization. For Shannon disorganized messages represented more information. For Wiener, entropy and information were opposite. The term “entropy” has been used in several scientific contexts. Often it is based on the concept of entropy proposed by thermodynamics, resulting equivalent to “disorder” (used in this way also by Norbert Wiener, the father of cybernetics mentioned before), sometimes, instead, understood as a measure of information complexity (according to information theory and so by Shannon).

It is clear there are different points of view: entropy can be seen as negative, but another way is to consider the information as negative or rather, differences in entropy correspond to differences in information of opposite sign.

On the other hand, it is clear how the SE is the amount of average information obtained after reading the message. So, it simultaneously goes to measure the degree of uncertainty before to read the message. It follows that the greater is the entropy, the higher the degree of unpredictability of a system, the greater the "disorder" in which it is (reasonable because the disorder has many more configurations of the few states that we call "ordered", therefore it is much more unpredictable). Consequently, it is more correct to say that differences in entropy correspond to differences in mean information of opposite sign. The latter corresponds to a change in what we know, on average, before and after the measurement.

2.2 Thermodynamic entropy and Shannon entropy

Everybody meets the term “entropy” for the first time approaching the second principle of thermodynamics. This principle is very generalizable, there are several statements of this principle and so, by extension, it has been used in different scientific contexts. The first field in which it born was the classic thermodynamic and the definition was made by R. E. Clausius in 1864. Entropy is an extensive quantity associated with a system in equilibrium. It is a quantity suitable for measuring molecular disorder. When the molecules are in a disordered system, it is more difficult to predict their position: the entropy will then be greater. For example, consider a gaseous state and a solid state. The entropy of the latter will certainly be lower because the particles cannot move from their equilibrium position but can only oscillate [24].

Considering two vessels, A and B, separed by a wall, caracterised by two entropy, respectively equal to S_1 and S_2. In the vessel A it is enclosed a gas while the other is empty (Fig. 2.3a). In this situation the entropys are constant and the state of A is ordered. When a hole is opened in the separation wall (Fig. 2.3b) , the gas spontaneously expands into the container B. This is an irreversible transformation and entropy increases by a quantity equal to:

$$S_2 - S_1 = \mathrm{R} \cdot \ln 2$$

Where R in the gas constant. In this situation the order of gas has decreased. It is also possible to say that the disorder has increased because the molecules try to occupy all the volume available in B (consequentially the entropy increases).

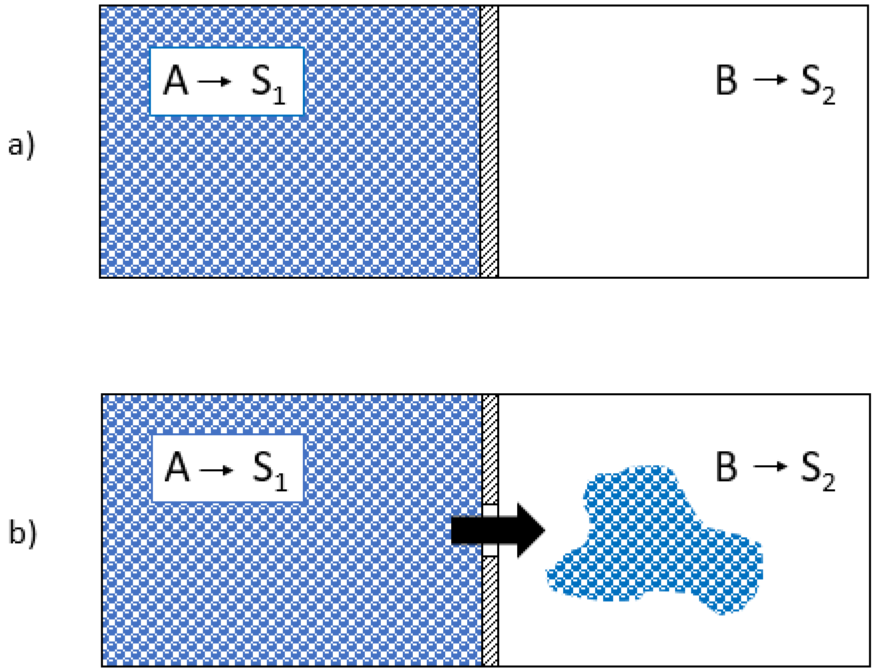

Figure 2.3: Two vessels, (A) with a gas, (B) empty. a) vessels separated by a wall, b) gas moving into B thanks to the opening of a gap in the wall.

Another field in which the entropy is applied is the statistical mechanics. It is the application of probability theory to the thermodynamic behaviour of systems composed of a large number of particles. The macro-state is the thermodynamic state of the system defined by values of different quantity as temperature, pressure etc. It is determined by the properties and by the motion of its microscopic components, as molecules, atoms and electrons. On the other hand, the microstates represent dynamic states that can be defined also knowing velocities and positions of all the system molecules. Statistical mechanics is able to connect the properties of the individual atoms and molecules to the macroscopic properties of the system it composes in order to make it unnecessary to consider the motion individually of each particle. At each state of macroscopic equilibrium, in fact, corresponds many possible states of microscopic equilibrium or molecular configurations.

Entropy is related to the total number of possible microscopic states of the system, namely the *thermodynamic probability p*, from the Boltzmann relation [16]

$$S = k \ln p \tag{2.5}$$

Where k is the Boltzmann constant ($1.38054*10^{-23}$ J/K) and p is the multiplicity of the possible configurations with which the particles of the system are distributed in the particular division (microstate) that corresponds to the state of the system (macrostate). From a microscopic point of view, the system entropy increases with the randomness and the indeterminacy of the position of molecules (molecular probability). It quantifies the probability that the particles are in one particular distribution among the many possible dynamic states in which they are they can be found. When an isolated system evolves spontaneously towards states of greater entropy, it is inclined to bring itself into the state that has a greater thermodynamic probability. The most probable macrostate is the one to which the greatest number of microstates is associated it is called “equilibrium state”.

It follows that entropy is a measure of molecular disorder and this one growths for every time that a transformation occurs.

Statistical entropy is reduced to Boltzmann entropy when all the accessible microstates of the system are equally probable. S is itself a thermodynamic property. Therefore, it acts as a link between the microscopic and the macroscopic world.

A generalization of Boltzmann entropy for all systems was made by Gibbs in 1902 because Boltzmann's entropy is considerable only if the systems are in global thermodynamic equilibrium, for an isolated system. Both entropy mentioned are a measure for microstates of a system, but the Gibbs entropy (Eq. 2.6) does not require that the system is in a single and well-defined microstate and exchanges energy with its surroundings.

For a system that is with probability p_i in a microstate, and being kb the Boltzmann constant, the Gibbs entropy is define as:

$$S_G = -k_B \sum_i p_i \ln p_i \tag{2.6}$$

Remembering the formulation of SE (Eq. 2.4), is possible to see that the Shannon, Gibbs and Boltzmann definition of entropy have close resemblance. Despite the foregoing, there are several differences. The first is the field of application. Shannon entropy, indeed, is used in information theory while Gibbs and Boltzmann entropy are used in statistical thermodynamics. Another difference consists in the role assumed by entropy: Gibbs entropy is the amount of chaos in a thermodynamically system, Shannon entropy is used within information theory that communicates the number of bits required to determine the outcome of a random process.

2.2.1 Maxwell’s demon paradox

It is now undeniable, at this step, that thermodynamics and information entropy are deeply related. The second law of thermodynamics affirms that any system, left to itself, switches spontaneously from order to disorder (because the latter is more probable), unless energy is supplied from outside. In 1871, the physicist J. C. Maxwell presented publicly in the book “Theory of heat” [25] a mental experiment that seemed to refuse the second principle. The main idea of Maxwell’s paradox is to have a creature capable of controlling a trapdoor that divides two containers that include the same gas at the same temperature (Figure 2.4). Within them there are faster and slower molecules. Whenever a high-speed molecule goes to the wall, the demon opens the trapdoor. After a certain period, all the fastest molecules are in one of the two containers and the slower ones in the other. Temperature is related with velocity, more the molecules are fast, higher will be the temperature. Then, the creature will be able to confine the hottest gas on one side and the coldest gas on the other, without converting a certain amount of work into heat.

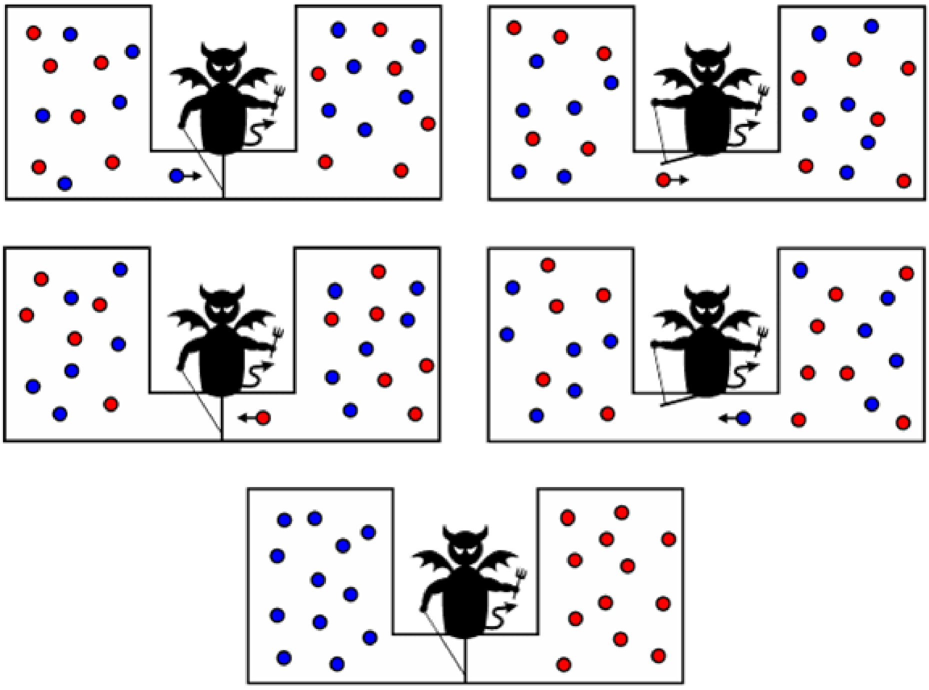

Figure 2.4: representation of the Maxwell paradox (Franco Maria Boschetto http://www.fmboschetto.it/tde3/termod7.htm) [26].

This "experiment" was in contrast with the second principle of thermodynamics that, in one formulation, affirms that it is impossible to transfer heat without converting a work into heat at the same time, how explained previously.

Many scientists tried to solve this problem. A solution of the Maxwell's demon paradox was suggested by Leo Szilard in 1929 [27] that formalized for the first time the relationship between information and entropy. Analysing the problem, he underlined that to measure the speed of the molecules Maxwell's demon would need to have some facility. Moreover, the acquisition of this information would require a waste of energy.

In 1961, Rolf Landauer [28] contradicted Szilard's idea because said that, if the measurement processes are reversible, they do not need to increase entropy.

His solution to Maxwell's paradox lies in the connection between thermodynamic entropy and information entropy. The Maxwell’s creature in fact, to decide whether to pass a molecule, had to have information on the state of the molecule. Deleting information caused dissipated energy. Moreover, this information could not be kept indefinitely by the demon.

In addition to the Landauer’s solution, Bennet, in 1982, showed that the demon, sooner or later, would have to erase information due to limited memory space. This action would have led to an increase in entropy and represented a thermodynamically irreversible phenomenon.

2.3 Application of information entropy

It is now evident that information entropy involves in different areas of research and that the concept of entropy could be extended to areas of application quite far from physics, first among everything the theory of information.

Recall that it equalized the degree of ignorance to disorder, considering the message as quantity of information which allows the receiver to move to a state of order or less uncertainty.

Therefore, the SE is employed in the theory of information to describe the level of complexity of a signal: higher is the Shannon Entropy, higher is the level of complexity necessary to recognize an information from another one when it is transmitted. In other words, the SE can be employed in order to understand how the signal is easy to forecast when, passing through an environment, it “leaves” information and interact with the environment.

The information entropy concept is used in different sectors: obviously in computer science, but also in biology, statistics, psychology and economics, to mention a few.

For this study, the fluids field was analysed, especially in terms of flow complexity and flow mixing but even to try to find a correlation with the fluid interactions with the environment (e.g. a fluid flowing in a channel). For the first, an interesting study has been carried out by Pozo et al. in 2017 [14] introducing an index (ICI, “interlacing complexity index”) based on Shannon’s mutual information (MI). Their aim was to investigate the flow complexity for open systems with inlet and outlet regions of arbitrary shape and topology. They have shown that the ICI provides a sensitive complexity measure underlining that the more complex the flow, the larger the information loss in the propagation from inlet to outlet.

The flow mixing, on the other hand, is commonly studied due to its relevance in many sectors, in both macroscale (e.g. mixing of gases in an engine) and micro scale (as microreactors and micromixers). To take into account the degree of mixing of some substances or fluids many approach are used. Camesasca *et al.* in 2006 [29] analysed this aspect precisely through the use of Shannon entropy. It assumed the maximum value (SE = 1) when the mixing was perfect, namely in any region the concentration of a component was equal to its concentration in the whole system. The minimum value (SE = 0) represented a state of perfect order, no loss of information and therefore no mixing between the species.

These examples of study confirm that information entropy is suitable to be use in numerous fields of study. For this reason, the new approach proposed in the present study (which will be explained in more detail in the next chapters) arises from the possibility that, within certain limits, the SE can be able to describe the nature of the environment with which a fluid has interacted only analysing the inputs and outputs of a channel. Considering the presence of some obstacles with different geometries in the channel, a question has been raised: analysing a laminar flow interacting with the obstacles, can the analysis of SE describe the nature of these obstacles?

This represents the scope of use of Shannon entropy theory in this research. Afterwards, when the study results will be discussed, the answer to this question will be provided.

Chapter 3

Materials and methods

3.1 Channel geometry

Starting from the idea to investigate the possibility to apply the Shannon Entropy analysis on the study of the fluid flow, and in particular on its interaction with the obstacles present, it was necessary to create the channel geometry. Moreover, the impossibility to solve the Navier-Stokes (NS) equations in presence of obstacles, the choice felt to describe the physic of the fluid employing a computational solver as FLUENT. The method required to create the model in ANSYS Workbench.

3.1.1 2D channel without obstacles

Considering the fact that this study based on Shannon Entropy was never proposed in literature, in order to verify the potential of the method, a simply first 2D configuration was explored.

The starting point was the study of a 2D parallels-plates channel without obstacles and it has been shaped as a rectangular channel with height 2h equal to 3 mm and length L* of 80 mm (Fig 3.1). The choice of this channel geometry derived by two aspects:

1. The field of application. The main ones are the microfluidic field. The channel constructed wanted to represent an ideal conduct of a microfluidic device.
2. Due to the low Reynolds numbers (Re) that characterize the fluid flows. In fact, with these values of Re the it flows at laminar conditions: the viscous effects are dominant on the inertial ones.

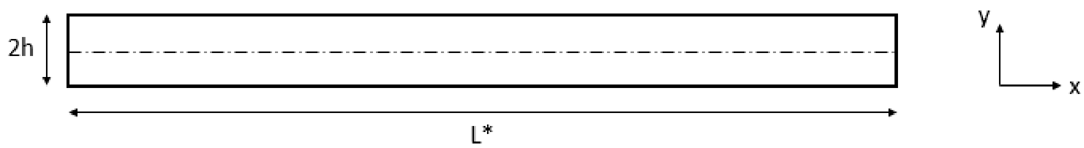

Figure 3.1: model of 2D channel without obstacles

The fluid flows from left to right. On the left there is the inlet of the channel while on the right there is the outlet.

Considering a fluid flowing in a channel/pipe, it is said to be one-, two-, or three-dimensional if the flow velocity changes in one, two or three dimensions respectively. However, if the velocity variation in certain direction is small relative to the variation in other directions, it can be neglected. In a circular pipe the development of the velocity profile is 2D at the entrance region, V=V(r,z), and became 1D downstream when the velocity profile fully develops and remain unchanged in the flow direction, V=V(r).

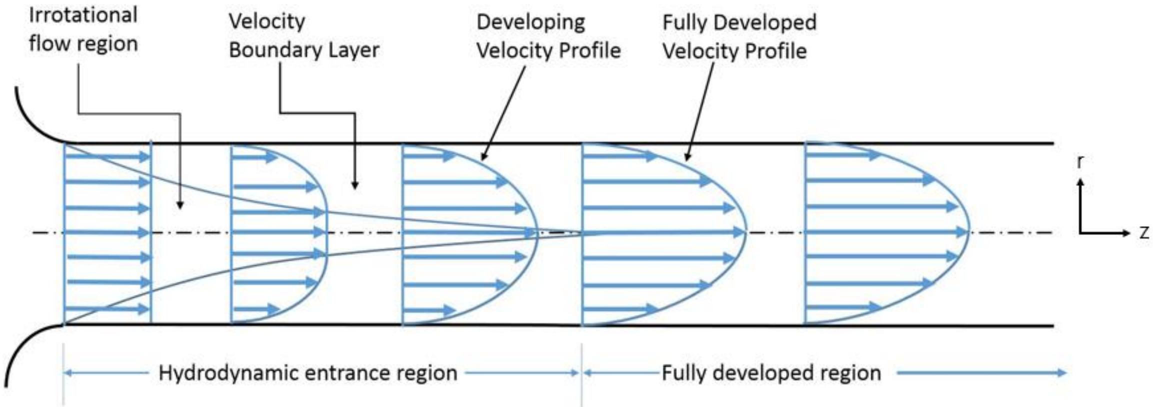

Figure 3.2: the developing velocity profile of a fluid entering a pipe. [30]

The analysis was carried out in the fully developed region in order to evaluate the velocity change when the geometry of the channel is modified, e.g. by the presence of an obstacle. This aspect will be discussed better in the next paragraph. The developing velocity profile of a fluid entering a channel can be evaluated with the relation (3.1) that takes into the account the value of the Reynolds number (Re) and the geometry of the pipe/channel. In particular the entrance length (Hydrodynamic entrance region in Figure 3.2) is define by:

$$\mathrm{L_d} = 0.05 \cdot \mathrm{Re} \cdot \mathrm{D_p} \qquad (3.1)$$

If the channel has a rectangular shape, D_p in (3.1) should be substituted using the concept of hydraulic diameter (3.2).

$$\mathrm{D_p} = \frac{4 \cdot \mathrm{A}}{\mathrm{S}} \qquad (3.2)$$

Where *A* represents the cross section of the pipe, *S* is the perimeter of the wet part of the channel. This verification is fundamental in order to confirm the condition of developed flow and to understand at which distance from the inlet the analytical solution (with a parabolic profile at laminar conditions) “exists”. In fact, the differential equations of continuity and of Navier-Stokes (N-S) can be solved by introducing simplifications. By means of the latter, is possible to obtain differential forms which can lead to approximate solutions. So, it is possible to divide the N-S equation to a linear differential equation. Therefore, in this way, the fully developed region can be described in terms of analytical representation.

To describe the laminar conditions, the physic of fluid mechanics employs no-dimensional parameter: the Reynolds number (Re). It is used to describe the transition from the laminar to the turbulent flow. It measures the ratio between the inertial effects and the viscous ones and it is described by the following formula:

$$\mathrm{Re} = \frac{\rho\ \bar{u}_x\ D}{\mu} = \frac{\text{inertial force}}{\text{viscous force}} \tag{3.3}$$

In this study, even the variability of the Re number was analysed. In fact, different values of Reynolds number have been considered. This variation is reflected in the L_d value. Seeing as how was necessary to compare different results changing the dynamic condition, it was necessary to verify, before the calculations, that the flow was completely developed independently from the increasing of the Re number.

To be sure that the flow is fully developed for every Reynolds number considered, the first 30 mm of the channel were never considered for the numerical and analytical solution of the velocity field. In this way, the real length of the channel is L_1=50mm.

3.1.2 2D channel with obstacles

Starting from the geometry depicted in figure 3.1, each small modification of the domain represents an “obstacle” in the solution of the N-S equations employed to describe the fluid flows. Obstacles were considered with different shapes and dimensions.

First of all, they were modelled using two different shapes: rectangular and semi-circular. The reason of this choice originated from the possible applications of the study. The idea was to trace back the profile of the obstacle to an elementary shape that could better approximate the possible shapes of obstacles in real cases.

Moreover, three different dimensions of the obstacles have been considered:

- $h_1 = \frac{h_{channel}}{10}$,
- $h_1 = \frac{h_{channel}}{6}$,
- $h_1 = \frac{h_{channel}}{2}$.

Other two parameters considered were the number of obstacles in the channel and their position, in the following configurations:

- One obstacle
- Two consecutive obstacles
- Two alternated obstacles
- One obstacle 5 times wider than the single one for the rectangular shape. In the semi-circular case, one obstacle 9, 7, 5 times wider than the single one respectively for $h_1 = \frac{h_{channel}}{10}$, $h_1 = \frac{h_{channel}}{6}$, $h_1 = \frac{h_{channel}}{2}$.
- Two symmetrical obstacles.

The different configurations were investigated for two Reynolds numbers: Re=1 and Re=50. Figure 3.3 shows the rectangular configurations that have been considered in the study. The same happened with the other shape investigated.

For rectangular obstacles their width L_1 was 0.5mm.

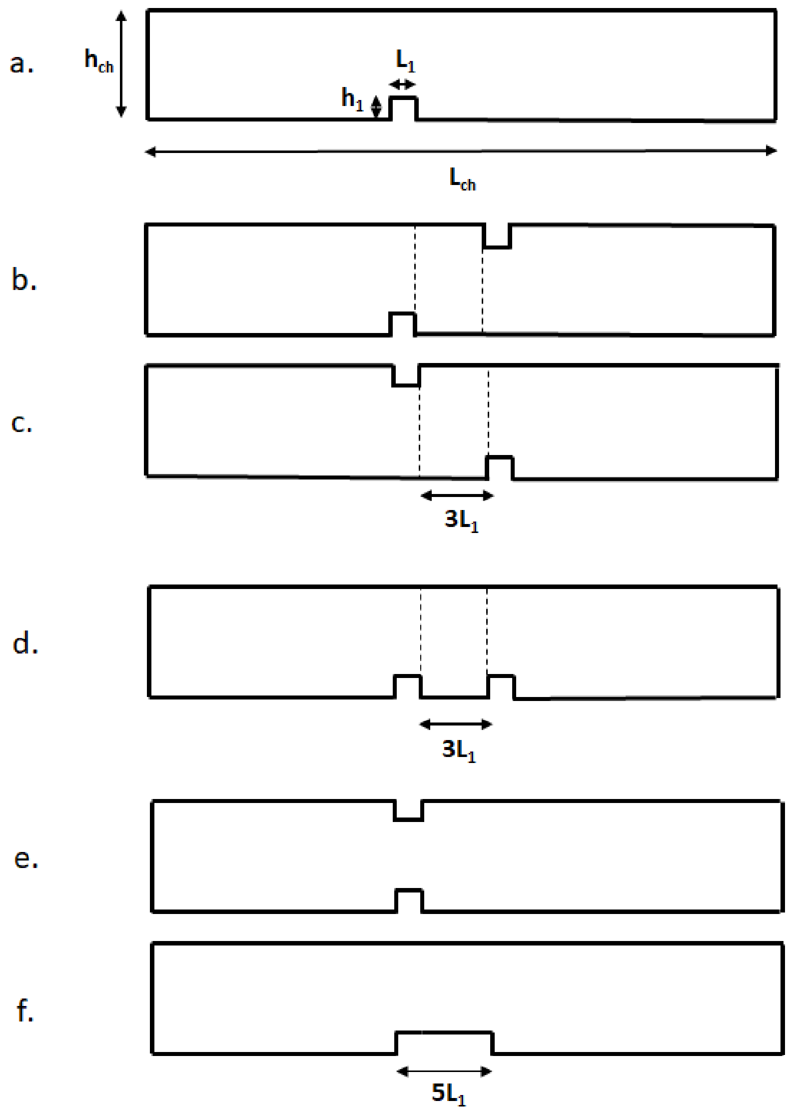

Figure 3.3: Rectangular obstacle: a) 1 obstacle, b) 2 alternate obstacles, c) 2 alternate opposite obstacles, d) 2 consecutive obstacles, e) 2 symmetrical obstacles, f) 1 extended obstacle.

For the semi-circular obstacles, given the nature of their geometry, was not possible to set a priori a width of the obstacles. In fact, if this were so, they would not be semi-circular but elliptical. For this reason, in order to make a comparison with the rectangular cases, the choice of the height of the obstacles was kept unchanged. In the case of semi-circular obstacles, the height is therefore equal to the radius of the obstacle. This dimension is also reflected in their width: the latter then becomes twice the radius (Fig. 3.4a)

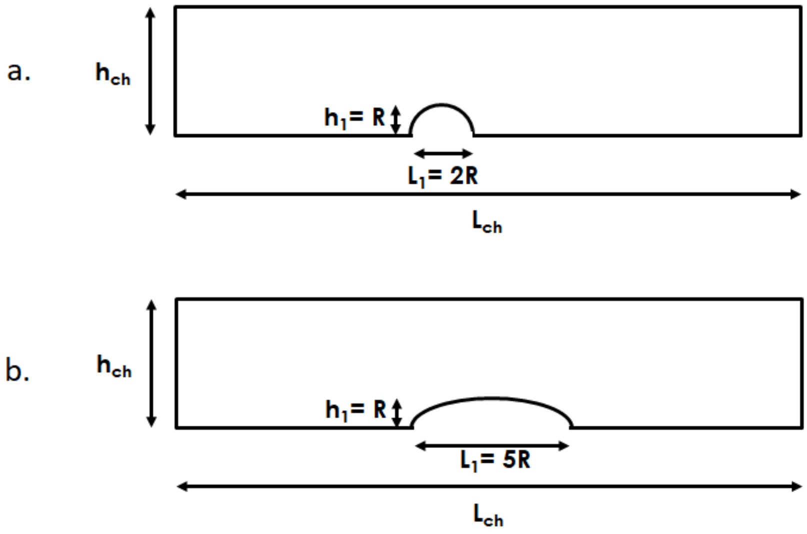

Figure 3.4: a) example of semi-circular obstacle, b) example of a semi-circular obstacle five times wider than the single obstacle

In the case of obstacle larger than the single one, for the semi-circular cases, because of the geometry of the obstacle, were not possible to consider the width equal to 2R. The construction of the obstacle changed depending on its height. The idea behind it was to investigate the differences between the cases *d.* and *f.* in figure 3.3. Then, the aim was to understand if, with the same width occupied in r-direction by the obstacles in both cases, there were differences between one single obstacle or two different obstacles. For this reason, the width L_1 in figure 3.4b was choose equal to the width in case of two consecutive obstacles. Then, for the semi-circular obstacles, the width was imposed equal to 9R, 7R, 5R respectively for $h_1 = \frac{h_{channel}}{10}$, $h_1 = \frac{h_{channel}}{6}$, $h_1 = \frac{h_{channel}}{2}$.

Even modifying the shape of the obstacles, position and configuration was maintained the same studied with the rectangular ones.

Investigating the case of two symmetrical obstacles, in order compare the results obtained with other configurations, the shape itself were modified too. In particular, the area occupied by the obstacles at the constriction level has been created preserving the total opening of the channel. In this way, in the symmetrical case, the single obstacle had a height equal to the half of the single obstacle. In figure 3.5 was depicted with a numerical example the construction of the symmetrical obstacles.

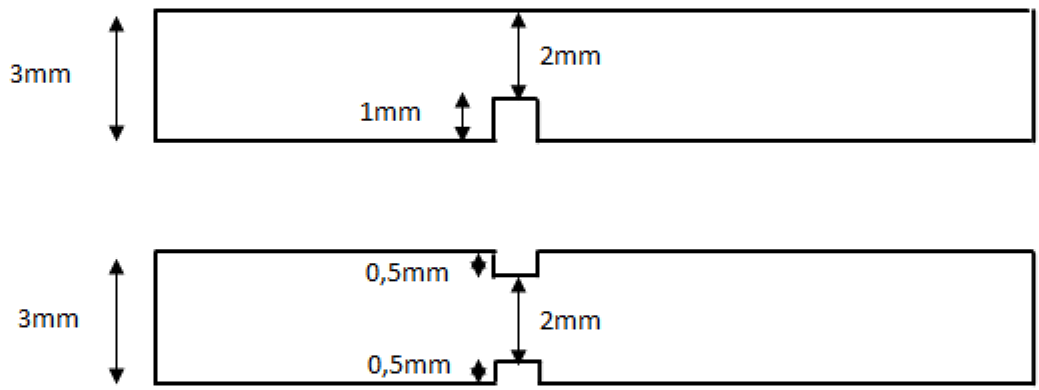

Figure 3.5: example of geometry construction of the case with two symmetrical obstacles.

On this way it was possible to compare the results obtained.

In order to carry out the analysis object of the study, to analyse the numerical results that will be discuss in the next paragraph, was necessary to divide the channels in three different sections to evaluate the areas in the proximity of the obstacles. Channels, as show in Figure 3.6, were considered divided in section 1 *pre-obstacle*, section 2 *with obstacle* and section 3 *post-obstacle*. Comparing the three sections, for example for the case with rectangular obstacles, on average, the first and the last section contain approximately 900 elements while the second between 15 and 75 elements. This large difference could be relevant in the numerical results. For this reason, the areas with the obstacle were never considered for the study due to the limit number of values that characterise this region.

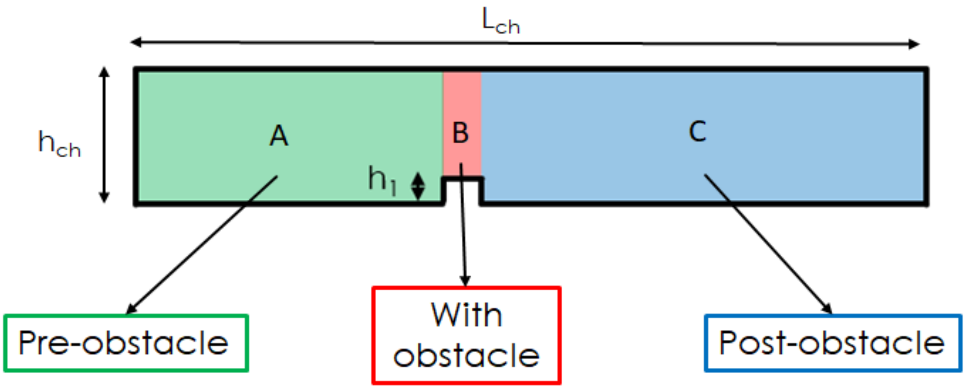

Figure 3.6: Partition of area in the channel: A) pre-obstacle, B) with obstacle, C) post-obstacle

B region was excluded because the numerical computation carried out to evaluate the Shannon Entropy was impossible without introducing a bias (if an error occurs, i.e. if SE values were equal to 0, given the few values in this section information would be assumed as undisturbed when maybe in reality it was not like that). Intuitively the B region is a filter through the fluid passes changing its dynamic.

3.2 Computational mesh

Each configuration was discretized with a grid, generated with ANSYS MESHING v.15.0. It was represented by quadrilateral elements in the whole domain. In order to obtain grid independent results, a mesh sensitivity study was carried out computing the maximum velocity at the centre of the channel for grids with higher and lower number of divisions. Secondly, the percentage difference between maximum analytical velocity (V_{max}^{ana}) and maximum numerical velocity (V_{max}^{num}) for each mesh size has been considered (Eq. 3.3).

$$\% \text{ error } = |\mathrm{V}_{\max}^{\text{ana}} - \mathrm{V}_{\max}^{\text{num}}| \cdot 100 \tag{3.3}$$

An error lower than 1% was considered and referred to the grid to employ obtaining a mesh independent model.

The grid dimension chosen consists of 24000 elements and 24831 nodes; the number of divisions was set up to 800x30 (channels had length and height of 80 and 30 mm respectively). For this grid the percentage error that comes from (3.3) was equal to 0,2%. A detail of the mesh (for the inlet section) is shown in Figure 3.7.

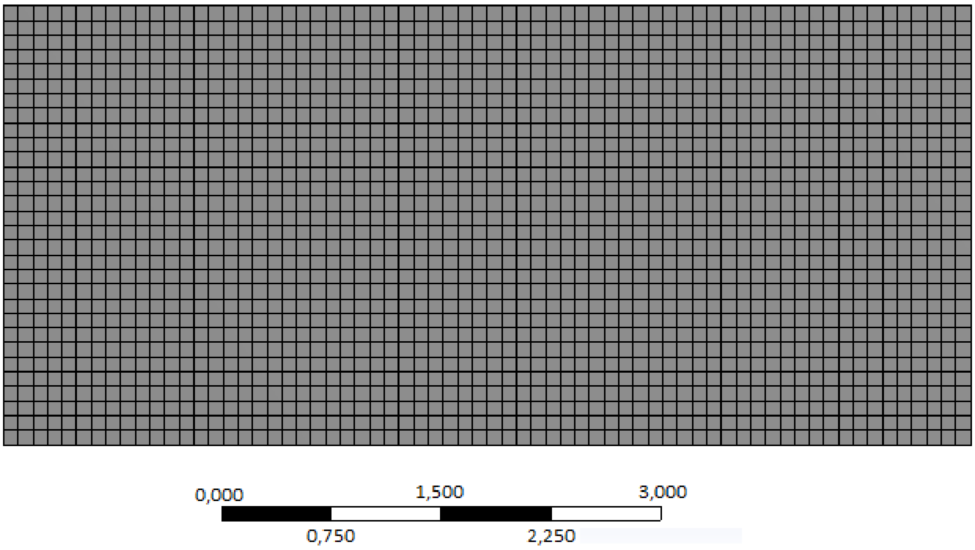

Figure 3.7: particular of the mesh grid

3.3 Numerical and analytical model

The fluid dynamics can be described through two principal equations: the conservation laws, in terms of mass, momentum and energy conservation, and with the continuity equation.

For incompressible flow with constant viscosity, the conservation of momentum can be expressed by the Navier-Stokes equations as follow:

$$\rho\frac{\partial\bar{u}}{\partial t}+\rho\bar{u}\cdot\nabla\bar{u}=-\nabla p+\mu\nabla^2\bar{u}+\rho\bar{g} \tag{3.4}$$

where

ρ = density;

μ = dynamic viscosity;

$\bar{u}$ = velocity;

p = pressure;

$\bar{g}$ = gravity constant;

For incompressible flow without chemical reactions, the conservation of mass can be written as, in vector form:

$$\nabla\cdot\bar{u}=0 \tag{3.5}$$

These two equations are the starting point to describe the dynamic of all fluids and they are able to describe every characteristic of the fluid. The main problem to solve the Navier-Stokes equations is the non-linearity of the convective terms $(u\cdot\nabla)u$ that make it impossible to determine analytical solutions.
For some cases, non-linear terms can be neglected, making possible to obtain the exact analytical solutions. In order to obtain it for the case analysed in this study, is possible to reduce the NS equations to a linear differential equation in the case of fully developed flow.

3.3.1 Analytical solution

For each case investigated is possible to solve the flow field numerically with ANSYS FLUENT®. For a channel without obstacle, is also possible to obtain the analytical solution of the velocity in a fully developed region, starting from the NS equations and solving them for a simplified phenomenon. Since the aim of the study was to carry out a re-construction of the characteristic of the environment where the fluid flows, when was possible, a comparison between the numerical solution and the analytical solution has been made. The latter was calculated for each case without obstacles, that is for Re=1 and Re=50, because in presence of obstacles was not possible to determine an analytical solution as discussed above.

First of all, was considered the solution for a two-dimensional flow between parallel plates [31]. Considering the distance between the plates equal to $2z_0$ (as shown in Figure 3.8), assuming that the velocity profile has a zero value in y and z direction, fluid develops only in the x direction (i.e. this is the condition for the fully developed flow). For this reason, only the equation relative to the x component of the momentum is considered, since the others have null terms. It can be written in the following form:

$$\frac{1}{\mu}\frac{\partial p}{\partial x} = \frac{\partial}{\partial z}\left(\frac{\partial u_x}{\partial z}\right) \tag{3.6}$$

Operating an integration and applying the following boundary conditions

$$\begin{cases} u_x = 0, & z = -z_0 \\ u_x = 0, & z = z_0 \end{cases} \tag{3.7}$$

with the suitable substitutions, it is possible to obtain the parabolic velocity profile for two parallels plates:

$$u_x = -\frac{1}{2\mu}\frac{\partial p}{\partial x}\left(z_0^2 - z^2\right) \tag{3.8}$$

Where

$$\bar{u}_x = \frac{2}{3}u_{max} = -\frac{1}{2\mu}\frac{\partial p}{\partial x}z_0^2 \tag{3.9}$$

$$\mathrm{Re} = \frac{\rho\ \bar{u}_x\ 2z_0}{\mu} \tag{3.10}$$

$$\frac{\partial p}{\partial x} = -\frac{\bar{u}_x\ 3\ \mu}{z_0^2} \tag{3.11}$$

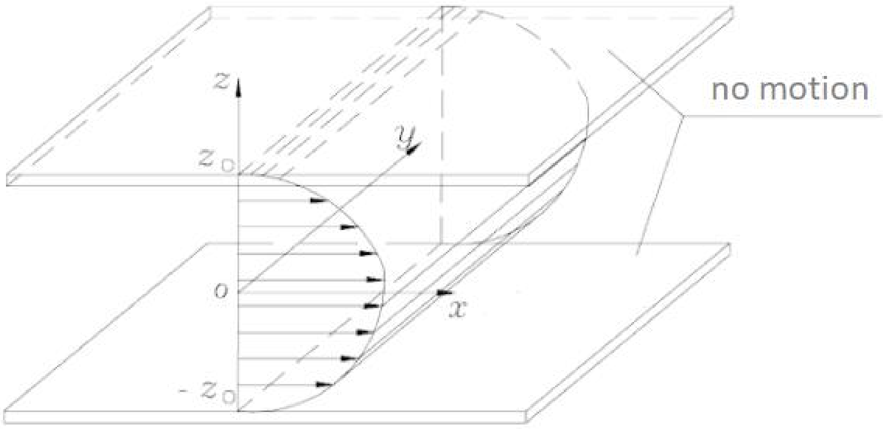

Figure 3.8: two-dimensional motion between parallel plates [32]

3.4 Boundary conditions for CFD simulations

To solve the velocity field in ANSYS FLUENT was necessary define boundary conditions to start the simulations. At the inlet of the channel, the velocity of the fluid was imposed. It was obtained by the relation (3.12) through the Re number, where D is the height of the channel (3 [mm]), μ the viscosity and ρ the density of the fluid considered. For this study has been chosen to work in laminar conditions and with very low numbers of Reynolds, in fact simulations were carried out considering Re=1 and Re=50.

$$\mathrm{Re} = \frac{\rho\ \bar{u}_x\ D}{\mu} \tag{3.12}$$

Inlet axial velocity was set to 3,30E-04 $\left[\frac{m}{s}\right]$and 1,67E-02 $\left[\frac{m}{s}\right]$respectively for Re=1 and Re=50.

For the simulations, water liquid has been chosen as the fluid of interest for the study. It is characterised by density ρ = 998,2 $\left[\frac{Kg}{m^3}\right]$ and viscosity μ = 10^{-3} $\left[\frac{Kg}{m\,s}\right]$. Moreover, flow was supposed unsteady and laminar. No *slip conditions* at the walls has been set.

For the solution methods, second order pressure discretization and second order upwind momentum discretization scheme were applied. The residual criterion to ensure the convergence of the numerical method was set to 10^{-6}.

In table 3.1 are summarised all the parameters that have been considered for the simulations; *Re* is the Reynolds number, u_x

	Case analysed	**Obstacle shape**	**Re**	**u_x [m/s]**	**Ana. solution**	**Num. solution**	$\frac{h_{ch}}{h_{ob}}$
1.	no obstacle	×	1	3,30E-04	✓	✓	×
2.	1 obstacle	rectangular	1	3,30E-04	×	✓	10, 6, 2
3.	2 consecutive	rectangular	1	3,30E-04	×	✓	10, 6, 2
4.	2 symmetrical	rectangular	1	3,30E-04	×	✓	10, 6, 2
5.	2 alternated	rectangular	1	3,30E-04	×	✓	10, 6, 2
6.	2 alternated opposite	rectangular	1	3,30E-04	×	✓	10, 6, 2
7.	1 extended	rectangular	1	3,30E-04	×	✓	10, 6, 2

8.	no obstacle	✗	50	1,67E-02	✓	✓	✗
9.	1 obstacle	rectangular	50	1,67E-02	✗	✓	10, 6, 2
10.	2 consecutive	rectangular	50	1,67E-02	✗	✓	10, 6, 2
11.	2 symmetrical	rectangular	50	1,67E-02	✗	✓	10, 6, 2
12.	2 alternated	rectangular	50	1,67E-02	✗	✓	10, 6, 2
13.	2 alternated opposite	rectangular	50	1,67E-02	✗	✓	10, 6, 2
14.	1 extended	rectangular	50	1,67E-02	✗	✓	10, 6, 2
15.	no obstacle	✗	1	3,30E-04	✓	✓	✗
16.	1 obstacle	semi-circular	1	3,30E-04	✗	✓	10, 6, 2
17.	2 consecutive	semi-circular	1	3,30E-04	✗	✓	10, 6, 2
18.	2 symmetrical	semi-circular	1	3,30E-04	✗	✓	10, 6, 2
19.	2 alternated	semi-circular	1	3,30E-04	✗	✓	10, 6, 2
20.	2 alternated opposite	semi-circular	1	3,30E-04	✗	✓	10, 6, 2
21.	1 extended	semi-circular	1	3,30E-04	✗	✓	10, 6, 2
22.	no obstacle	✗	50	1,67E-02	✓	✓	✗

23.	1 obstacle	semi-circular	50	1,67E-02	×	✓	10, 6, 2
24.	2 consecutive	semi-circular	50	1,67E-02	×	✓	10, 6, 2
25.	2 symmetrical	semi-circular	50	1,67E-02	×	✓	10, 6, 2
26.	2 alternated	semi-circular	50	1,67E-02	×	✓	10, 6, 2
27.	2 alternated opposite	semi-circular	50	1,67E-02	×	✓	10, 6, 2
28.	1 extended	semi-circular	50	1,67E-02	×	✓	10, 6, 2

Table 3.1: parameters evaluated in the study

3.5 Methods for analysis

When in a channel the fluid meets an obstacle, the fluid particles change their trajectories because the fluid try to adapt itself to the new geometry. This variation depends by different factors (e.g. fluid velocity, viscosity etc.) including the dimension of the obstacles. If a fluid is influenced by the environment, the question that could be considered the starting point of this study was: may the variation of the flow become source of information of the entire system? May the fluid be analysed as source of information?

How said in chapter 1, only few and recent studies posed this question, sometime in different way [13] [14].

In particular in these pages the idea was to correlate the dimension of the obstacles with the fluid motion in order to understand at which conditions the presence of the obstacle influences the behaviour of the fluid.

To achieve this goal, the approach was to extract information about the transformation of the system analysing a quantity wide employed in thermodynamic to describe every kind of phenomena and its evolution in time. This quantity is the well-known terms called entropy, but not in the thermodynamic sense, rather in an informative sense by the concept of Shannon entropy (SE).

3.5.1 Evaluation of Shannon Entropy

As mentioned in chapter 2, a fluid that flows in a channel brings information; it is a carrier (e.g. the blood in our body carries information and nutrients). So, if a fluid can be considered as a reservoir of information and if this information can be analysed to take out useful info, the challenge is to understand in which way it is possible to exploit this "thermodynamic" resource. The aim of the study is to deepen about the exploitation of this fluid intrinsic information, carrying out a re-construction of the characteristic of the environment itself where the fluid flows.

The SE was taken up by Claude Shannon in 1948 [1] when he applied the concept to information theory, in order to describe the level of complexity of a signal in the field of data communication system (see chapter 2).

For this reason, a parallelism with a fluid that flows in a channel will be proposed in this study, considering as a transmitter the inlet of the channel and as a receiver the outlet, while fluid is the information transmitted. A schematic representation is shown in figure 3.9.

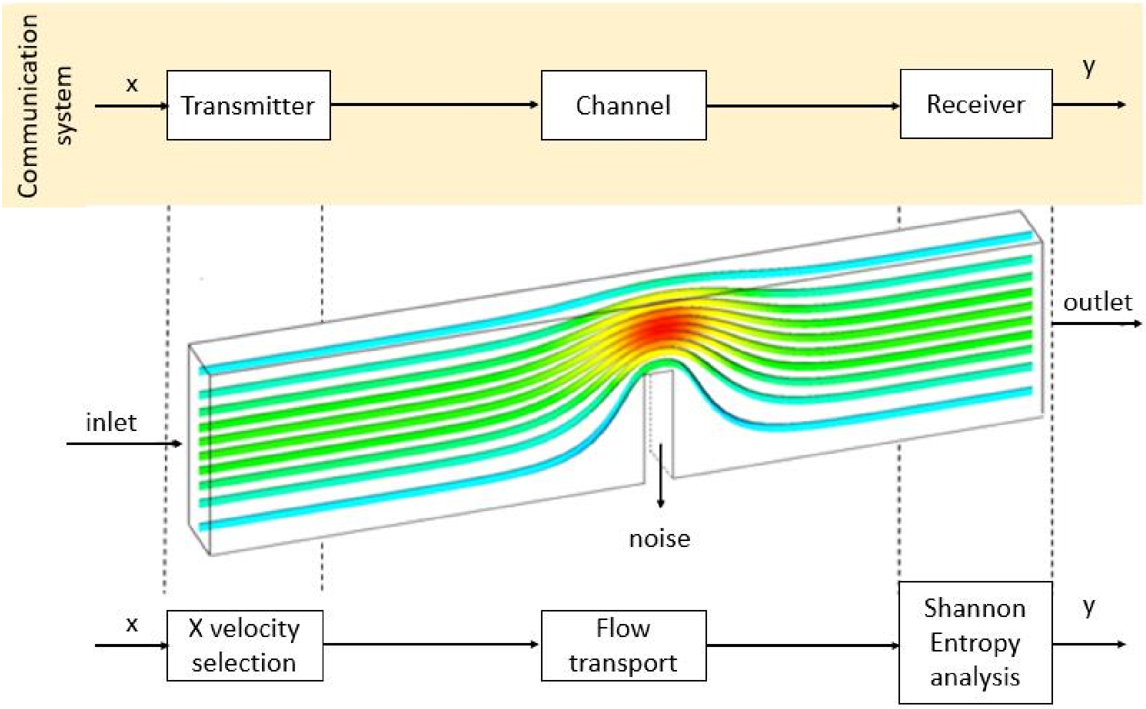

Figure 3.9: parallelism between a communication system applied and a fluid that flows in a channel.

When SE is employed in the information theory, it describes the level of complexity of a signal: higher is the Shannon Entropy, higher is the level of complexity necessary to recognize an information from another one when it is transmitted. In other words, the SE can be employed in order to understand how the signal is easy to forecast when, passing through an environment, it "leaves" information and interact with the environment. To better understand the meaning of SE, it is necessary to remember the main idea of this theory. A message with a low value of probability carried more information, *vice versa*, if the probability is higher it has less information and consequently its entropy is lower.

Considering a coin throw in which the probability that the result is heads or tails is the same, the entropy value (that have a range of 0 ÷ 1) is equal to 0.5 because the two events have the same probability equal to 1/2. This situation is affected by uncertainty. Instead, if it is known that the coin is altered and there are two heads, the entropy is equal to 0 due to fact that the results will be always heads, so the outcome can be predicted perfectly.

The idea is linked to the fact that if the fluid flowing in a channel, meeting structures such as obstacles, it adapts itself to geometry during motion, so the particles change their trajectories. From a thermodynamic point of view, this behaviour can only influence the internal energy of the system and consequently entropy. It can be expected an increase in entropy when in the interaction zone the fluid runs into obstacles because the motion of the system change and became more unpredictable, more disordered. As a matter of fact, entropy would seem to have all the characteristics to be a descriptor of the state of a system when it modifies its configuration.

Coming back to the Shannon Entropy [1], by definition its formulation is represented by equation 3.13.

$$S(X) = -P(x_i)\ \log_2 P(x_i) \tag{3.13}$$

Where, X is a discrete random variable with possible values $\{x_1, \ldots, x_n\}$ while $P(x_i)$ is a probability distribution of X, it represents the probability that the x_i event occurs. The increase of entropy corresponds theoretically to an increase in information loss. This aspect will be discussed in detail in the following paragraphs.

3.5.2 Binary matrix of velocity

Depending on the field of application $P(x_i)$ can take into account different variables. To analyse the fluid field there are several fluid dynamic parameters on which it is possible to focus attention as velocity, density, pressure etc that can be evaluated with different tools. In this study, in order to calculate the information underlying the application of Shannon entropy calculation, it was decided to operate on the velocity vector.

From literature there are not many studies on this matter. However, Pozo *et al.* [14] analysed flow complexity in open system, therefore studied more complex phenomena and with a greater amount of data, but going to study at a level information the variation of the streamlines in a channel.

In fact, usually, to describe a flow field and therefore how the fluid flow effectively, is necessary to visualize it graphically. There are different ways to achieve the aim, the main means that are generally used are: streamlines, pathlines and streaklines [33].

- Streamlines: family of curves that are tangent to the flow velocity vector or the flow direction at every point in the flow field instantaneously.
- Pathlines: trajectories that individual fluid particles follow. Fluid particles are marked with a dye and then observed as they move.
- Streaklines: locus of positions of the fluid particles marked that at some earlier instant passed through a fixed point of space.

In this study the starting point, to employ the SE according with the intentions of the study, was to consider a channel in which the fluid flows at laminar conditions, as already discuss in chapter 3. By reference to figure 3.10, only sections "pre-obstacle" and "post-obstacle" have been considered for the numerical results because the width of the obstacle is very small compared to the others. In fact, obviously, where the obstacle is present there are not values of velocity calculated. In order to avoid the occurrence of errors due to lack of speed values where the obstacle is present, this region has been neglected in this study (section "B" in the figure 3.10).

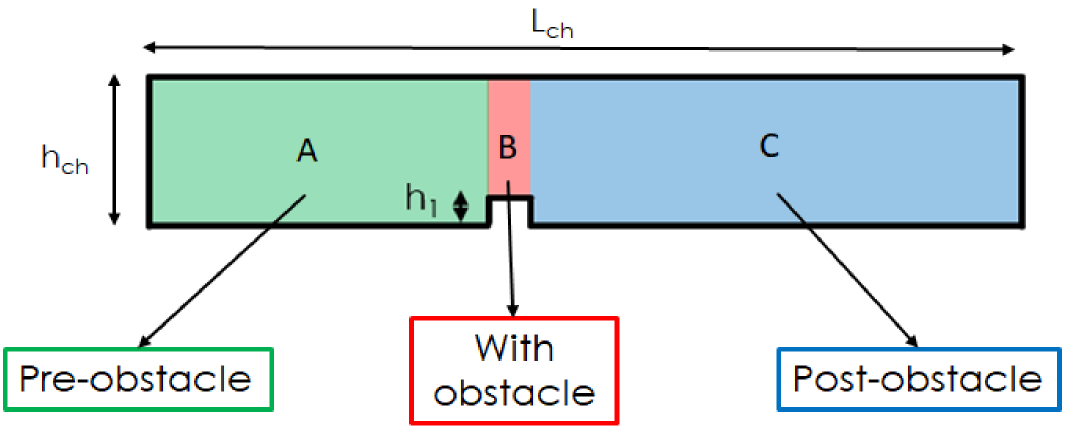

Figure 3.10: Partition of area in the channel: A) pre-obstacle, B) with obstacle, C) post-obstacle

Knowing that without obstacles the streamlines must follow a linear path, this scheme has been used as starting point: any obstacle is able to modify the "message" in input. The message used as reference was built using a binary matrix of velocity where all elements were equal to 1 to describe parallel streamlines. As mentioned above, the streamlines connect all the points having the same velocity and in channels with smooth walls at laminar conditions all the particles follow paths parallel to the walls. This scenario corresponds to the case of channel without obstacles in its whole domain (figure 3.11).

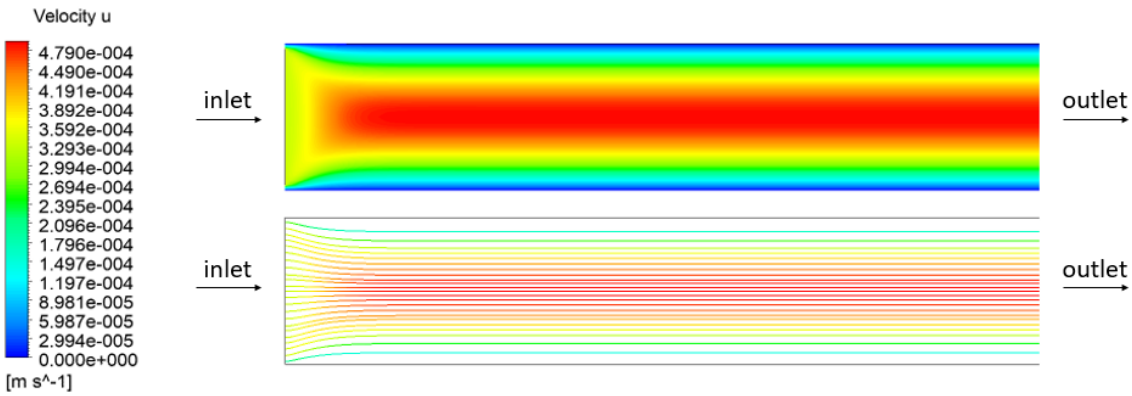

Figure 3.11: representation of contours and streamlines for a channel without obstacles in the whole domain.

If a changing of the channel geometry occurs, even though maintaining laminar conditions, a fluid follows different paths and the streamlines leave their parallelism. But if the streamlines undergo a variation, even the content of the matrix must show a change, its elements will be not all equal to 1.

To perform the analysis of the SE, once to have reach the convergence of the numerical simulation, position coordinates and velocities were exported from FLUENT along the whole channel. Figure 3.12 shown a schematization of the channel with the reference coordinate system considered.

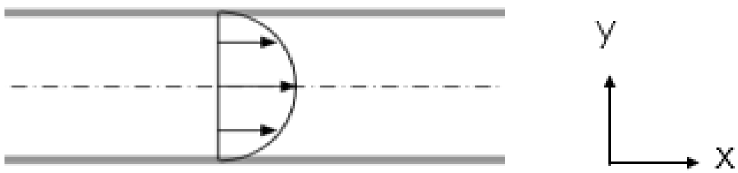

Figure 3.12: reference system

Therefore, a binary velocity matrix alongside the x coordinate (axis of the channel) has been constructed. Considering the matrix row by row, in each cell of the row the difference between the ratio of velocity of a x component and its previous value was computed, and the ratio of the analytical velocity in the same positions was evaluated. Namely:

$$B_{i,j-1}^{x} = \begin{bmatrix} b_{1,1} & \cdots & b_{1,j-1} \\ \vdots & \ddots & \vdots \\ b_{i,1} & \cdots & b_{i,j-1} \end{bmatrix} \tag{3.14}$$

in which the value of the binary elements of the matrix was calculated as follows:

$$b_{i,j-1} = \begin{cases} 1, & \dfrac{u_{i,k}^{x}}{u_{i,k-1}^{x}} \leq const \\ 0, & on\ the\ other\ cases \end{cases} \tag{3.15}$$

The *const.* value comes from analytical solution, discussed in a previous paragraph (equation 3.8), comparing the velocities values at the same coordinates:

$$\frac{u_{x}^{num.}}{u_{x-1}^{num.}} - \frac{u_{x}^{ana.}}{u_{x-1}^{ana.}} = const \tag{3.16}$$

Where $u_{x}^{num.}$ and $u_{x}^{ana.}$ are respectively the numerical and analytical velocity values, while $u_{x-1}^{num.}$ and $u_{x-1}^{ana.}$ are the same variables but in the previous x position. All values discussed above are calculated in the case without obstacles.

Considering the case without obstacle as a reference of undisturbed situation, if in the simulation the velocity changed faster than the case without an obstacle or if the velocity change did not follow a linear behaviour due to the presence of obstacles, the behaviour of the fluid was different than the case without obstacle and so it was necessary to consider the phenomenon: we were in one of the "other cases" of the relation 3.15. In these cases, indeed, the fluid flowed with the influence of the obstacles and so it adapted itself to the new geometry causing a variation in its motion: its velocity varied.

Therefore, the matrix thus constructed included only values equal to 1 or 0. The sum of ones, from the binary matrix just obtained, was computed for each row (equation 3.18). The matrix dimension depends by the number of cells considered. For the case analysed, the sections “pre-obstacle” and “post-obstacle” (figure 3.10) never had the same number of cells due to the different dimensions of the obstacles. The maximum value of sum represented the sum “undisturbed”, namely the sum that would be in the case without an obstacle. In this case, indeed, because the matrix contained only “1” value since the velocity never changed in the whole domain, the sum could only take the maximum value. It depended by the number of cells in the case under examination.

The ratio between the above-mentioned parameters, identify the probability present in the definition of the Shannon entropy (equation 3.17) because:

$$S = -p_i \log_2 p_i \tag{3.17}$$

$$p_i = \frac{sum\ of\ ones}{sum\ max} \tag{3.18}$$

The result of the binary matrix construction was a vector of SE values (between 0 and 1) equal to the number of rows of the mesh. The choice to carry out the study under binary conditions was arbitrary. In the next future is not excluded the possibility to employ others numerical codes in function of the dynamic conditions.

The outcomes of the analysis, for each case analysed discussed at the beginning of this chapter, were two different binary matrices referring to the “pre-obstacle” and “post-obstacle” sections.

So, when the fluid flowed in a channel in absence of obstacles, the calculus brought to obtain a matrix when all values were equal to 1. When the behaviour of the fluid was far from this condition, the binary matrix changed and even the SE assumed different values.

Remembering what was said about the streamlines, the configuration in which streamlines were parallel lines represented the lowest level of SE or the most coherent condition in which the fluid flowed without losing information. With a SE=0 the information was transmitted without interferences and the inlet information is formally equal to the outlet. When a modification occurred and, for example, an obstacle generated an interference, the SE assumed a value that was expected to be ≠ 0 with a maximum of 1 (equation 3.19). The fluid dynamics result to be different from the analytical solution of Poiseuille’s flow. Always referring to the interpretation of the SE as a measure of the complexity of an information, higher was its value, higher was the complexity of the fluid movement and the inertia effects were much more influent on the fluid behaviour.

$$S = -p_i \log_2 p_i = \begin{cases} 0, & \text{no information lost} \\ 1, & \text{information lost} \end{cases} \tag{3.19}$$

An important step was to understand what SE meant and how could be employed to this problem of fluid-mechanic.

3.6 Average entropy and centre of distribution

An example of a graphical representation of the SE vector is shown below:

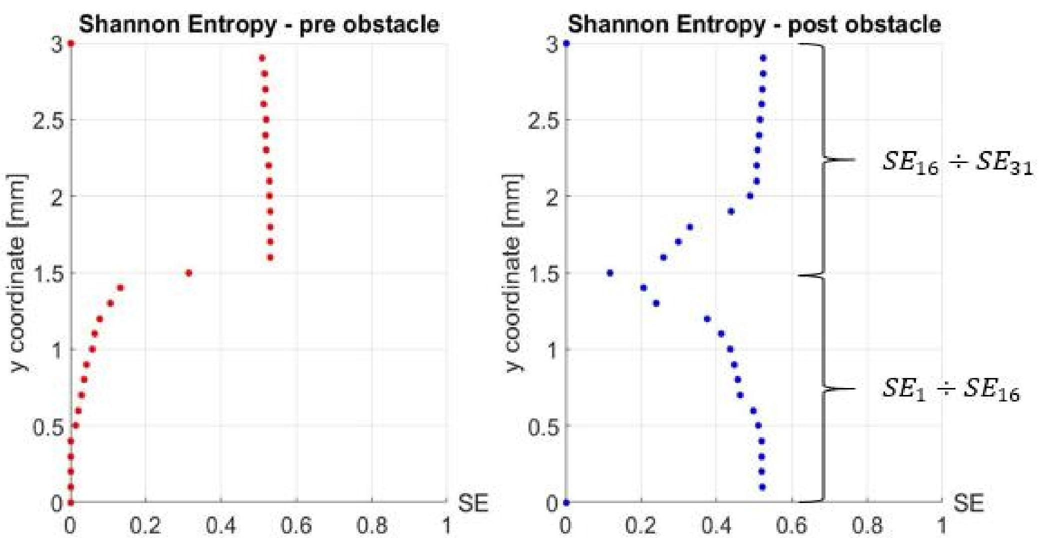

Figure 3.13: example of SE trend.

In order to investigate the distribution of SE in the channel, other two parameters have been calculated from the SE vector:

1. Average SE
2. Centre of distribution of SE

The first was calculated on the x axis by the following formula:

$$\text{Average SE} = \frac{\sum_{i=1}^{31} M_i \cdot \ SE_i}{\sum_{i=1}^{31} M_i} \tag{3.20}$$

Where M_i represents the mass that in this case it has been assumed equal to 1. The number of SE values resulting from the numerical simulation was 31. This value derived by the number of cells in the mesh size. The average SE represented the distribution of the SE values respect to the minimum and the maximum value that the SE could be assumed, 0 or 1.

Instead, the centre of distribution y' was calculated on the y axis by the following formula:

$$y' \cdot \left(\sum_{i=1}^{16} SE_i\right) = \left(\sum_{i=16}^{31} SE_i\right) \cdot (3 - y') \tag{3.21}$$

Mainly:

$$\text{Centre of distribution} = \frac{3 \cdot \sum_{i=16}^{31} SE_i}{\sum_{i=1}^{31} SE_i} \tag{3.22}$$

Remembering that the channel was high 3 mm, $SE_1 \div SE_{16}$ represent the values of SE in the inferior half of the channel, from 0 to 1.5 mm, whereas $SE_{16} \div SE_{31}$ the superior half, from 1.5 to 3 mm (Figure 3.13). This parameter was investigated to analyse where the SE is more influent in the y coordinate. In other words, the aim of studying these two parameters was to investigate the distribution of SE in both x and y coordinate in order to characterise spatially the value of SE.

An example of representation of the average SE and the centre of distribution is shown in the following figure. In Appendix A will be show all the results about this analysis.

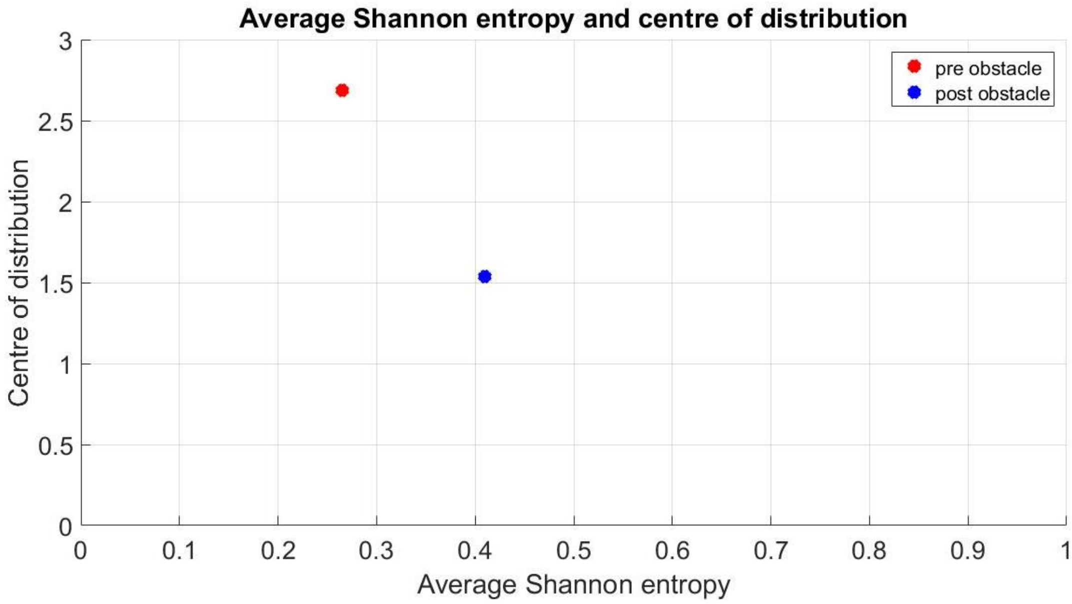

Figure 3.14: example of average Shannon entropy and centre of distribution

Chapter 4

Results

How explained in chapter 3, the numerical cases analysed were a lot, for this reason was necessary to identify which were more significant in order to underline the information given by the Shannon entropy analysis. For the analysis of results, an obstacle/s height of $h_1 = \frac{h_{ch}}{6}$ has been considered and the cases that has been chosen were the following:

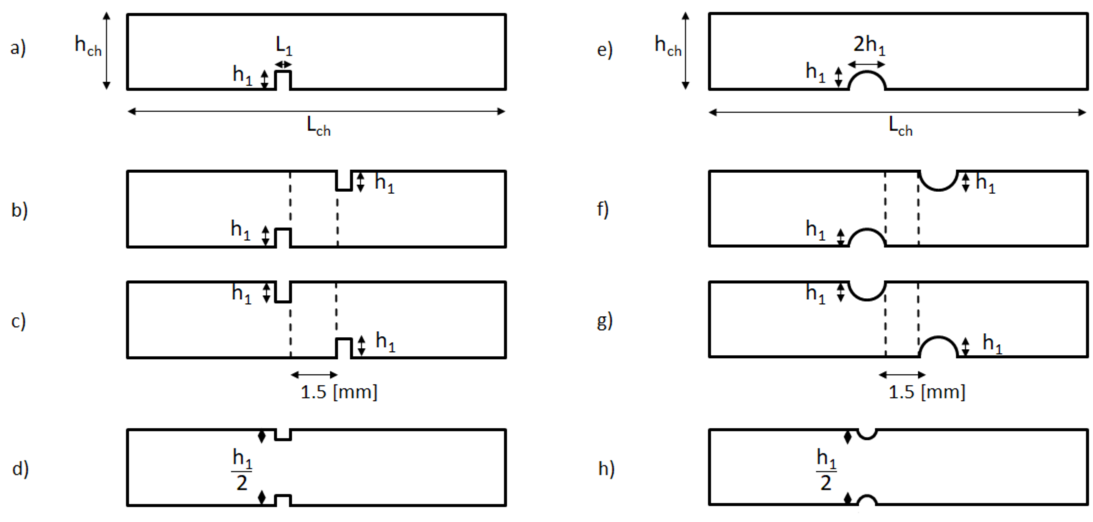

Figure 4.1: Rectangular obstacle: a) 1 obstacle, b) 2 alternate obstacles, c) 2 alternate opposite obstacles, d) 2 symmetrical obstacles. Semicircular obstacle: e) 1

obstacle, f) 2 alternate obstacles, g) 2 alternate opposite obstacles, h) 2 symmetrical obstacle.

These choices have been done essentially for two aspects. The first is because better represent the situation in a hypothetic real case, namely those that could potentially be found within a real channel. The second is since presented mainly the differences between the different configurations in order to make a comparison in shape, dimension and multiplicity.

For the case *d.* and *h.* in figure 4.1 is necessary to remember that the area occupied by the obstacles at the constriction level has been created preserving the total opening of the channel. In this way, in the symmetrical case, the single obstacle had a height equal to the half of the single obstacle. This aspect shows the first critical issues in the study. Indeed, was necessary to decided how to operate in order to make a comparison between different configurations. The problem was that, in the realty, for any value of radius, the area of the rectangular obstacle cannot never be equal to the area of the semicircular obstacle. For example (figure 4.2), consider the rectangular configurations and suppose to fix the height of the obstacle equal to 1 [mm] and the width to 0.5 [mm]. If you wanted to reproduce the same situation but considering a semicircular obstacle, keeping the height equal to 1 [mm] unchanged, you would of course have a width of 2 [mm]. Indeed, the latter corresponds to twice the radius, i.e. the diameter. The two areas are different, in particular for the area of the rectangular configuration is equal to 0.5 [mm^2] while or the semicircular obstacles is equal to 1.57 [mm^2].

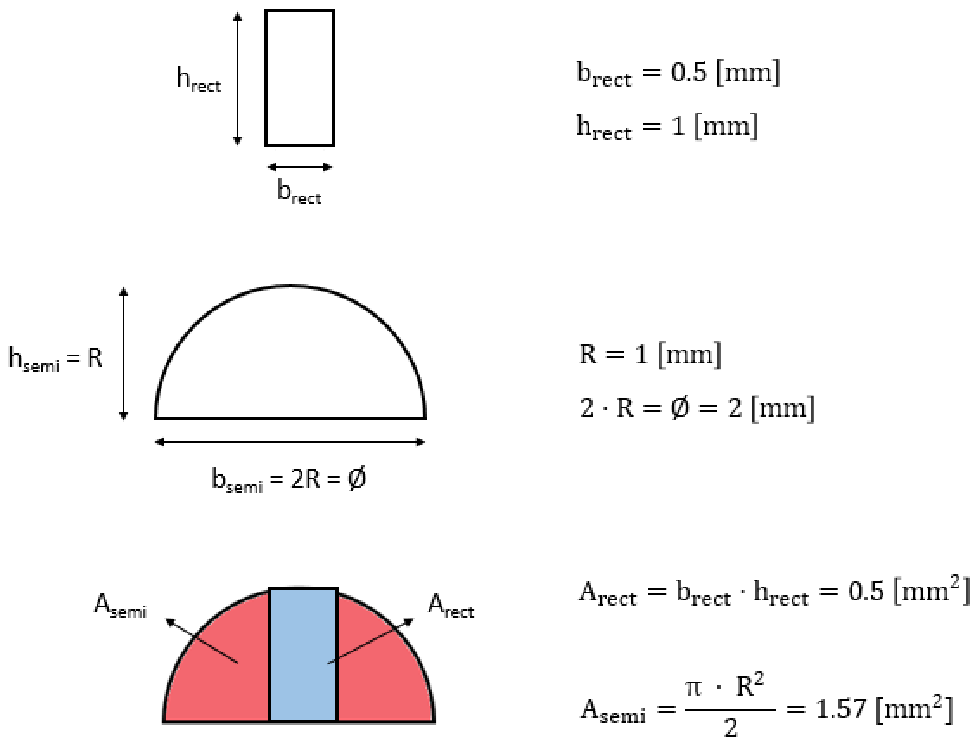

Figure 4.2: example of different areas for rectangular and semicircular obstacle.

Due to the impossibility of having equal areas, the choice fell on maintaining unchanged the height of the obstacle in the two different configurations. The height of the rectangular obstacle corresponded to the radius of the semicircular obstacle.

Make a comparation between obstacles with two different shapes can be useful for characterise the response of Shannon entropy (SE) curve, since it was expected to present two different trends. On the other hand, if we want to evaluate the variation of the latter, we must however consider that the different geometries taken into account already imply a greater intrinsic variability in the curves due to the different shape of the obstacles.

It can probably be more useful to compare configurations that have the same obstacles shape, for example the cases *a.* and *d.* (figure 4.1) in which the fluid flows in the same section. Considering the same obstacles shape, at the same number of Reynolds (Re) and area occupied, it can lead to a variation of the SE and therefore one could blindly understand the geometry that characterizes the channel. It could consequently be useful to understand if inside the geometry changes (e.g. inside a scaffold for cell growth).

For the analysis of the results, the *Re* number was important. In this study were taken into account two different values: *Re*=1 and *Re*=50. It is now necessary to summarise what the no-dimensional *Re* number means. It is used to describe the transition from the laminar to the turbulent flow. It measures a ratio between the inertial effects and the viscous ones.

$$\mathrm{Re} = \frac{\rho \cdot \bar{u} \cdot D}{\mu} \tag{4.1}$$

Where:

ρ = density of the fluid.

$\bar{u}$ = average velocity.

D = characteristic length, in this case is the height of the channel.

μ = dynamic viscosity of the fluid.

It is well known that at low Re numbers the fluid flow is laminar. At this condition, the viscous effects are dominant on the inertial ones. From another point of view, while is flowing, the fluid maintains a certain level of coherence and particles follow precise paths. For example, at Poiseuille conditions, in a pipe such as that one presented in figure 4.3a, the particles that are carried by the fluid follow a linear path, and the information is transmitted from the inlet section to the outlet one following the scheme depicted. On the other hand, in panel b of the same figure, the particles path in presence of a turbulent flow is shown to highlight the difference with respect to the case of laminar flow.

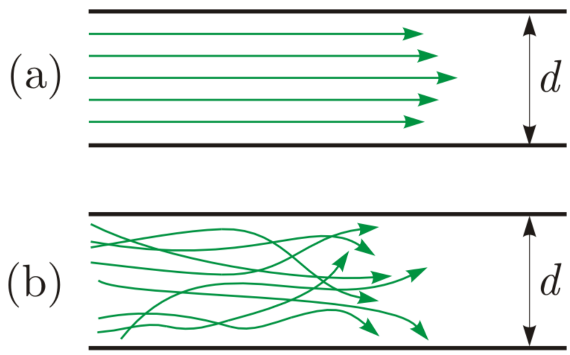

Figure 4.3: (a) laminar flow, the particles follow a specific path; (b) turbulent flow, the particles follow casual paths. For the first case, in each section is possible to be sure from where a particle is coming.

The equation 4.1 tells that when Re is higher than pre-determined value the inertial effects are dominant. At these conditions the fluid moves in a stochastic way passing from a foreseeable flow to a casual one. No forecast can be done.

The viscous effects tend “to make us forget” the external influences on the fluid; i.e. the flow is influenced by the porous medium at different levels from the interface till the deeper regions far from the free fluid flow. From another point of view, the viscosity tends to uniform the behaviour of the flow reducing the discrepancy between the free flow and the one at the porous medium level.

Viscosity can be considered as a way with which a fluid dissipates its energy, losing the information obtained during the interaction with the environment. The inertial effects, on the other side, make more “efficient” the propagation of the perturbations, playing an opposite role if compared with the viscous ones.

From this interpretation came the idea that a fluid can be considered as a reserve of information and consequently the idea of applying information theory to describe the nature of the environment in which the fluid flows, analysing the "information carried" in different sections of the conduit (chapter 2).

For all the reasons described above it is now clear the great dependence of SE to the *Re* number. a modification of the latter, and therefore of viscosity, can probably lead to variations in the SE. Given its importance, for the purpose of the study it is necessary to investigate what happens by changing the number of *Re*. For this reason, this aspect will be mentioned later as future development.

All the numerical analyses were carried out in order to understand if the aim predetermined at the beginning of the study could be reached. In fact, in this chapter will be present the results obtained from the simulation and the post processing of the data.

It will be explained if the SE analysis is able to provide a reconstruction of the internal geometry of the channel by discriminating the different configurations listed at the beginning of the paragraph and diversifying the presence of obstacles in disposition, geometry, size and multiplicity. To achieve this purpose, several evaluations have been made and several SE analyses have been conducted in parallel, all of which will be shown and explained in the following paragraphs.

4.1 Obstacles rectangular VS semi-circular

The first comparison was made between the cases with rectangular and semicircular obstacles in the same configurations, in order to determine if the SE can be discriminating in the case of different obstacle geometries. For this analysis the following cases have been chosen, both at *Re*=1 and at *Re*=50 and for a height of channel equal to $\mathrm{h}_1 = \frac{\mathrm{h}_{\mathrm{ch}}}{6}$:

- One obstacle.
- Two symmetrical obstacles.
- Two alternated opposite obstacles.

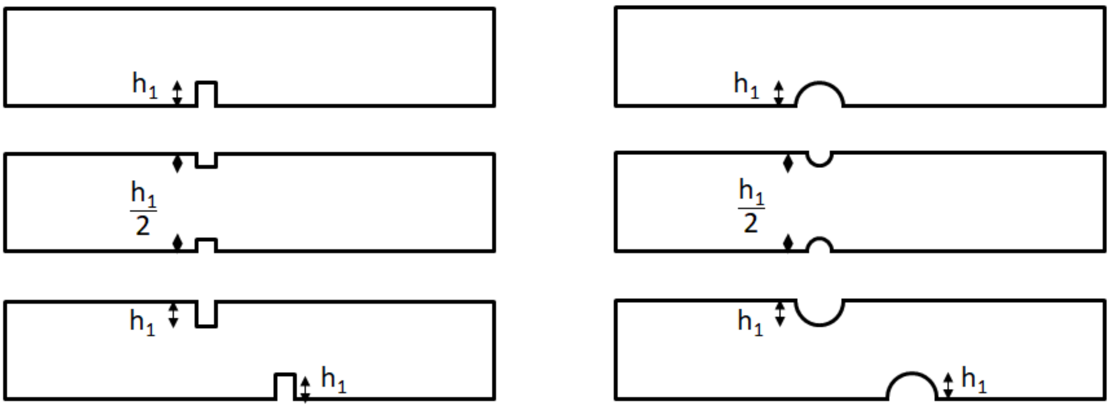

Figure 4.4: Comparison between obstacles rectangular and semicircular. a) one obstacle, b) 2 symmetrical obstacles, 3) 2 alternated opposite obstacles.

For all these cases the SE curve has been obtained and plotted in the “pre” and “post” sections (as discussed in chapter 3):

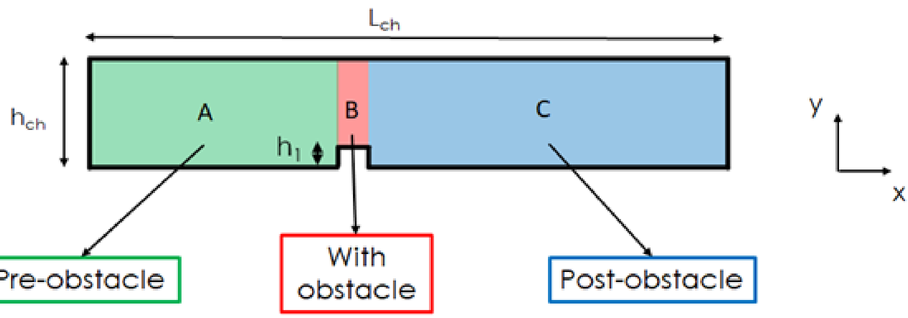

Figure 4.5: Different sections of the channel.

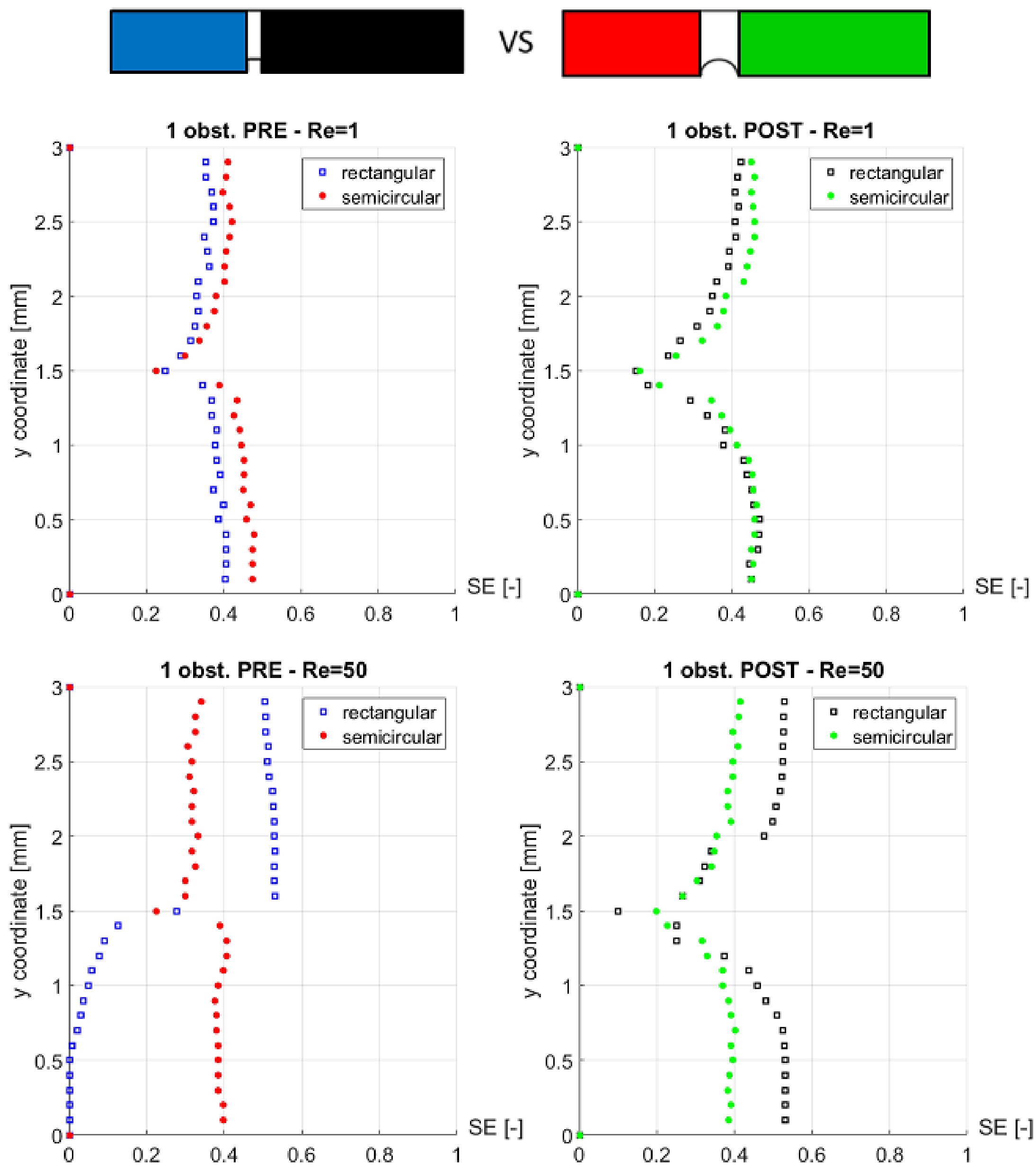

Figure 4.6: SE trend for one obstacle rectangular and semicircular at Re=1 and Re=50.

In figure 4.6 is possible to see how, at *Re*=1, the curves appear more similar in trend and values assumed. Instead, at *Re*=50 the SE trends are different. In particular, in the "pre" section of a rectangular obstacle, the SE seems to discriminate between the two geometries. Looking the plot is also possible to see that the SE assumes a value not null in correspondence of the obstacle height (0.5 [mm]).

In case of two symmetrical obstacles (figure 4.4b) it was expected to find this symmetry in the curve of the SE. If so, it would be able to give a large amount of information about their disposition. The following figure shows the SE result for two symmetrical obstacles, rectangular and semicircular, always for *Re*=1 and *Re*=50.

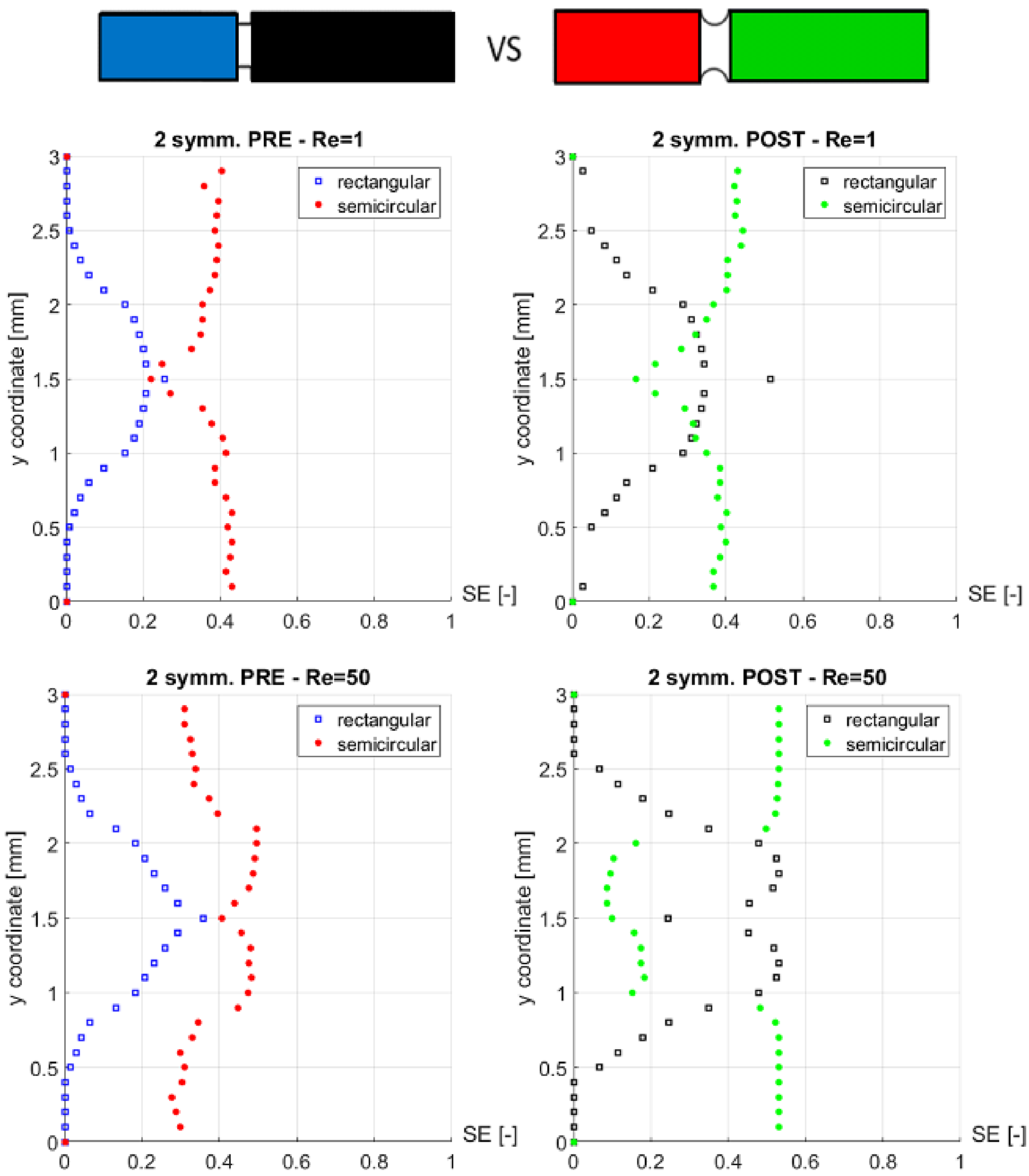

Figure 4.7: SE trend for 2 symmetrical obstacles rectangular and semicircular at Re=1 and Re=50.

The symmetry of the obstacles to different *Re* numbers is evident in both geometries but, particularly in the rectangular-shaped obstacles in which symmetry is perfect.

Another feature to underline is the difference in the trend of the curves for the two different geometries. In fact, both at *Re*=1 and at *Re*=50, we can notice how the SE curves differ considerably from each other. This is a very positive aspect because, if we knew the type of SE response to a certain geometry, we could know (without having knowledge of the internal geometry of the channel) what kind of obstacles are present within it.

It is possible to notice that in this case, the value of SE for semi-circular obstacles is greater than the SE of rectangular obstacles. For the case with two symmetrical obstacles at *Re*=50, in “pre” section, semi-circular configuration is well represented by the trend of the SE. in fact, near the walls of the canal, it is possible to notice how it approximates the shape of the obstacle encountered by the flow in its path.

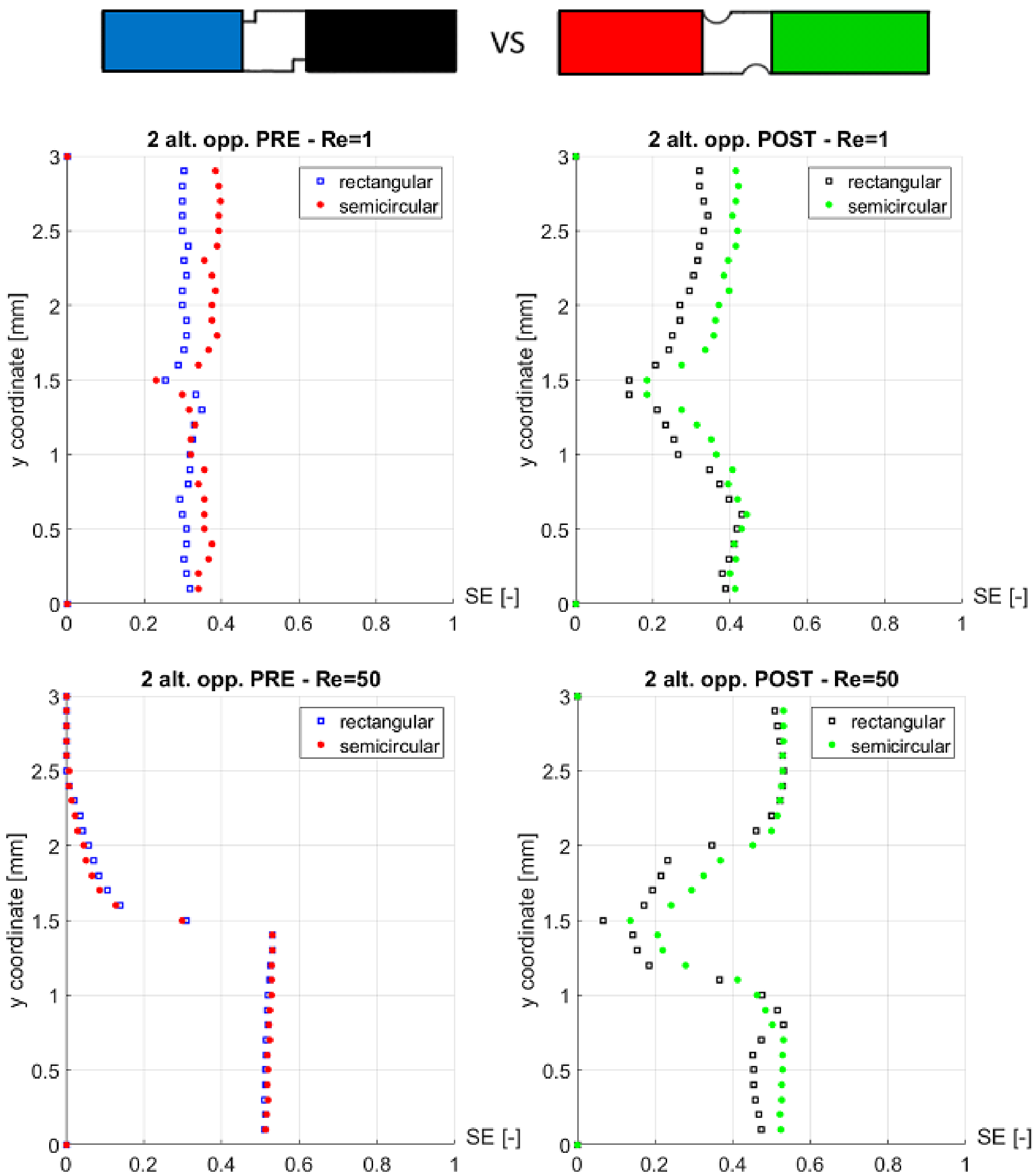

Figure 4.8: SE trend for 2 alternate opposite obstacles rectangular and semicircular at Re=1 and Re=50.

In the case of alternated obstacles, the SE curves in the rectangular and semicircular case are very similar, both as a trend and as assumed values. In one case (figure 4.8, “pre-Re=50”) they coincide almost perfectly. In this case, therefore, the SE seems to be not very able to discriminate between two different geometries. Compared to the case with two symmetrical obstacles, it is also possible to highlight the difference in similarity. In this situation in fact, there is no evidence of the disposition of the obstacles, except for “pre-*Re*=50” in which can be seen that the first obstacle that the fluid meets is in the superior wall of the channel.

4.2 Different number of point for the SE definition

For the calculation of SE, the previous analyses were conducted considering a number of points equal to the number of elements of the grid. In this analysis it was chosen to consider only the 50% of points considered in the previous investigation. Also for this investigation, the SE has always been calculated in the two sections "pre" and "post" obstacle (figure 4.5), with a height of obstacles $h_1 = \frac{h_{ch}}{6}$ and it was carried out for the configurations shown in figure 4.10.

This evaluation has been conducted to understand if it was possible, for application purposes, to reduce the number of sections analysed: in order to verify if less information about the velocity of the fluid in the channel would be sufficient. The 50% of the points to analyse have been chosen in three different ways.

Primarily, both velocity values in the “pre” and “post” obstacle, at Re=1 and Re=50, were considered choosing alternate elements of the grid (green and sky-blue elements in figure 4.9a, white were excluded from the calculation).

In order to select the set of elements other two tests have been executed: the first test took into account all the elements that had been neglected in the previous ones, therefore the white columns were considered instead of the green and blue ones (figure 4.9a). Whereas, in the second trial, the average value of SE between two consecutive columns has been taken into account (red dots in figure 4.9b). If the columns in “pre” and/or “post” obstacle were of odds numbers, then it was chosen not to consider the first column (inlet of the channel) in the case of the “pre” obstacle section and/or the last column (outlet of the channel) in the case of odd “post” obstacle section. The reason of this choice was related to the fact that points farer from the obstacle had less influenced by the latter ones.

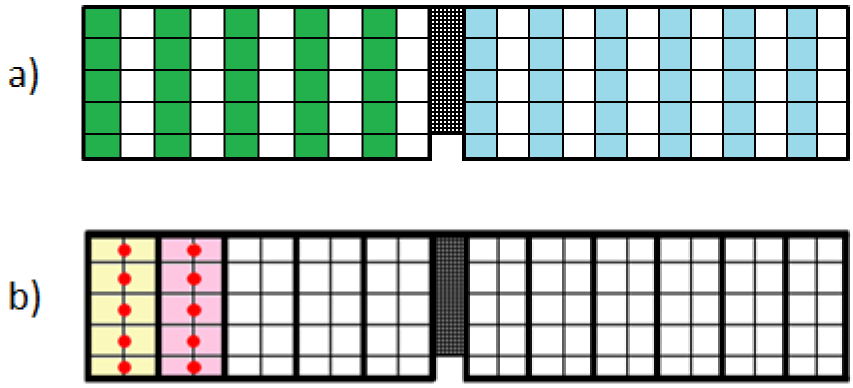

Figure 4.9: Grid elements chosen for the analysis with the 50% of point of SE. a) elements chosen for the first and second method, b) mean value of SE in two adjacent columns.

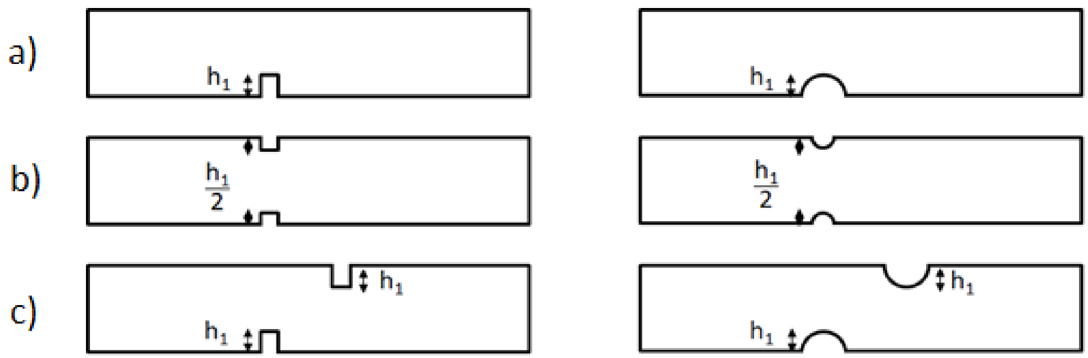

Figure 4.10: Comparison between obstacles rectangular and semicircular. a) one obstacle, b) 2 symmetrical obstacles, 3) 2 alternated obstacles.

The reason why it was chosen to carry out these two other tests was due to the need to verify if the choice of the elements, part of the 50% considered, could be decisive in the production of the result. Subsequently, the three methods described above will be compared so as to highlight any differences.

As presented at the start of this chapter the idea behind this analysis was to reduce the number of points evaluating the SE in order to understand if there was a minimum number of points to analyse to carry out the study. Decreasing the number of points, indeed, it is possible to expect an influence on the SE trend such that it is necessary to consider a minimum number of points to analyse.

There are therefore two key ideas: the first is that it should not be possible to extrapolate information in a section too poor of points; the second is that a certain number of sections are sufficient to carry out the analysis. The latter factor can be of great interest because it would allow to be able to consider only certain coordinates and not the whole domain, therefore it represents a lower cost and a lower need of resources. The problem was that decreasing the number of points automatically increases the uncertainty of the measure. The purpose is precisely to quantify this uncertainty so as to know the minimum number of resources needed.

The results obtained with the analysis of the SE considering the 50% of the points are shown below. They are compared to the SE calculated on the entire grid or considering 100% of the points. What was expected was to find the same trend of the SE, probably with slightly different values, which therefore were not too discrepant from the results shown in paragraph 4.1.

In the following figures will be present the results obtained by the comparison of the SE trends considering both 100% and 50% of points. For the latter, first of all, were considered the values relating to the first method described (green and sky-blue elements in figure 4.9a has been selected). Then were evaluated also the other two methods described.

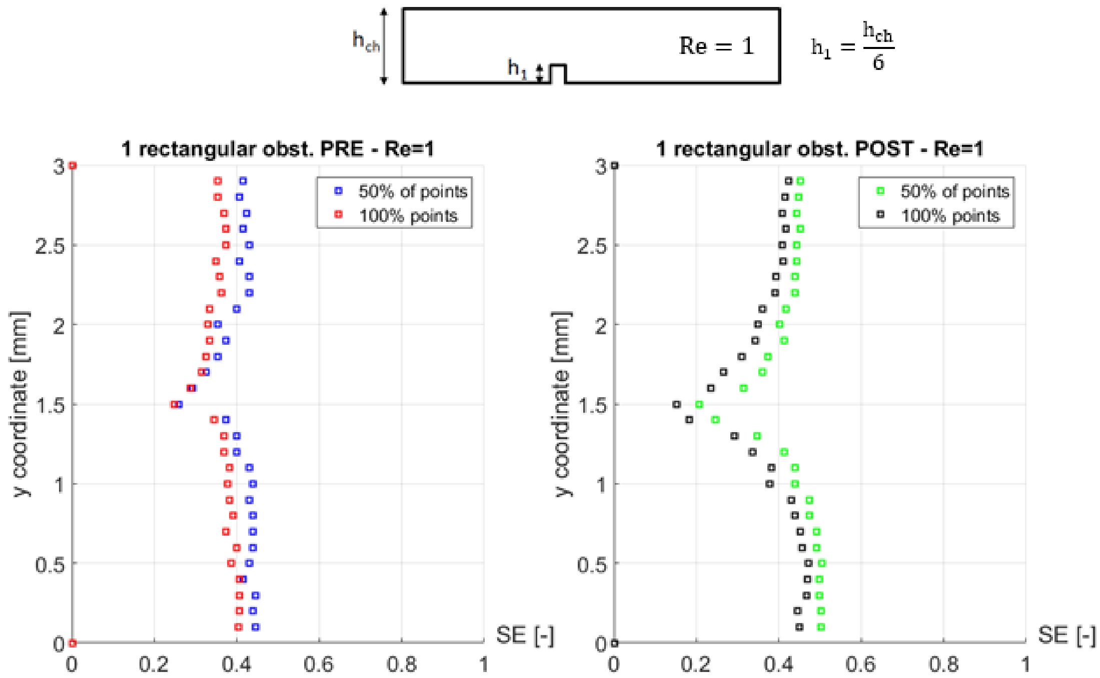

Figure 4.11: Comparison between SE calculated in the whole grid and SE calculated considering the 50% of points for one rectangular obstacle in “pre” and “post” section at Re=1.

Among all the configurations examined, the configuration with one rectangular obstacle at Re=1 is one in which the values of SE considering the 50% of the points deviate more from those calculated on the entire grid. However, it is noted that both the “pre” and “post” trends that the values assumed are very similar (identical situation even in the semicircular case, figure 4.12).

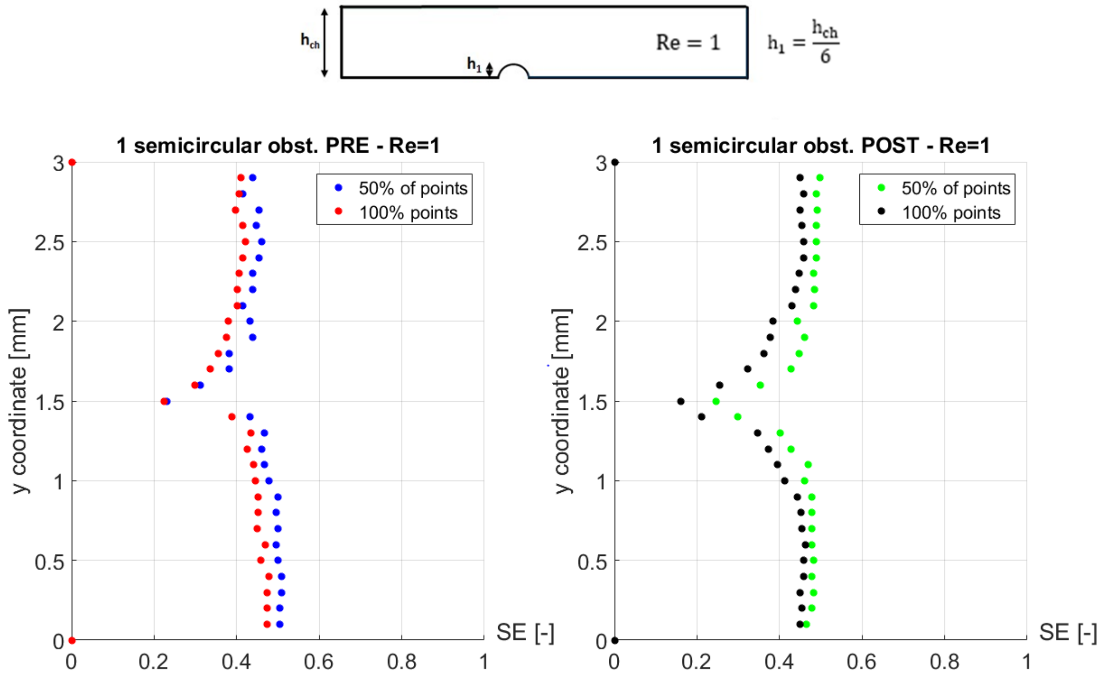

Figure 4.12: Comparison between SE calculated in the whole grid and SE calculated considering the 50% of points for one semicircular obstacle in "pre" and "post" section at Re=1.

It is also possible to see that the average entropy increases when the 50% of points is considered. It was an expected result because, considering half of the points, the uncertainty of the measure increases, less information is present and therefore entropy will be greater, according to the concept of information entropy (Chapter 2). This result is positive because the differences between the two cases analysed for the "pre" and "post" section were very small.

For every configuration, a quantification of error between each method has been made in order to define the maximum that can occur. Considering the next equations, the quantification of error was computed as follows:

$$\mathrm{Err}_{\mathrm{pre\%}} = \mathrm{mean}\left(\left|\mathrm{SE}_{\,100\%\_\mathrm{pre}} - \mathrm{SE}_{\,50\%\_\mathrm{pre}}\right|\right) \cdot 100 \tag{4.2}$$

$$\mathrm{Err}_{\mathrm{post\%}} = \mathrm{mean}\left(\left|\mathrm{SE}_{\,100\%\_\mathrm{post}} - \mathrm{SE}_{\,50\%\_\mathrm{post}}\right|\right) \cdot 100 \tag{4.3}$$

Considering the one rectangular obstacle at *Re*=1 configuration, for the “pre” section it was obtained an error equal to $Err_{pre\%}$ = 3.9% while, for the “post” section, it was equal to $Err_{post\%}$ = 4.6%.

Afterwards, the values assumed by the SE were compared considering the whole domain, 50% of the points (described above) and 50% of the points considering the opposite columns of the grid ("50% of points-opposite", white elements in figure 4.9a).

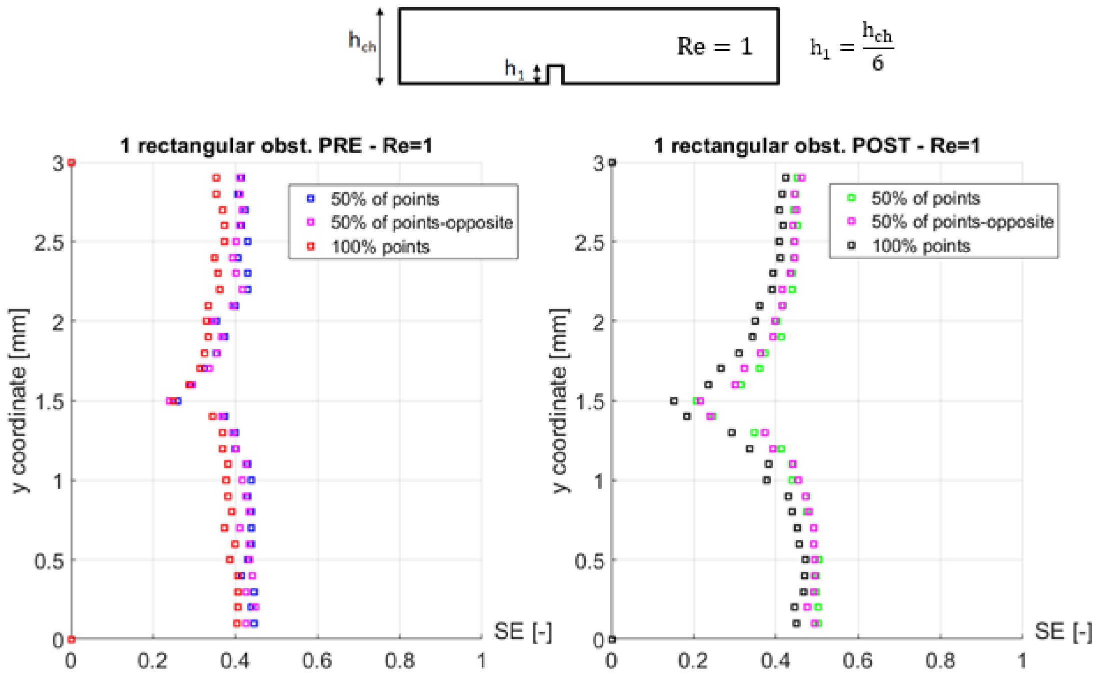

Figure 4.13: Comparison between SE calculated in the whole grid, SE calculated considering the 50% of points (green and sky-blue) and the opposite 50% of points (white elements) for one rectangular obstacle in “pre” and “post” section at Re=1.

This comparison shows that between the two different SE calculations considering 50% of the points there is not a substantial difference. The SE, as in the previous situation, maintains its trend and the values differ little from each other. This difference will be quantified as follows to assess whether it can be considered acceptable or not. Taking into the account the same definition of error for “pre” and "post" sections explained in equation 4.2 and 4.3 the results show that between the two different methods to calculate the 50% of point there are errors equal to $Err_{pre\%,1}$=1% and $Err_{post\%,1}$=0.97% respectively for "pre" and "post" sections. Instead, considering as touchstone the SE value for the 100% of points, the error between this value and the latter 50% method explained is equal to $Err_{pre\%,2}$=3.37% for the "pre" section and $Err_{post\%,2}$=4.15% for the "post".

Compared to the previous case the error values are slightly lower. The difference between the two errors is however so low that it is possible to neglect it and to suppose that, for this moment, the choice of the elements of the domination does not infect the measure too significantly. In this study, an in-depth analysis of the error between the different methodologies was not made. Surely this is an aspect that should be analysed because it could be significant for the results, will therefore be proposed as a future development.

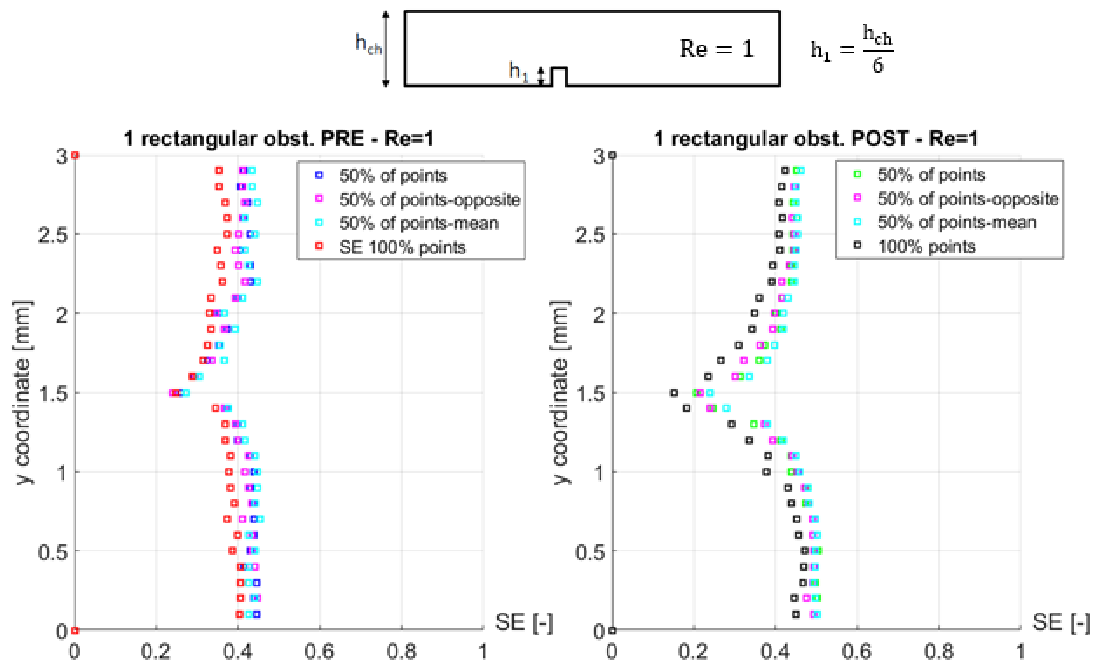

Figure 4.14: Comparison between SE calculated in the whole grid, considering the 50% of points (green and sky-blue), considering the opposite 50% of points (white elements) and averaging between two adjacent columns for one rectangular obstacle in "pre" and "post" section at Re=1.

This analysis puts in evidence that the SE trends are more similar in all the cases. On the other hand, there is always a little difference between the different cases. How done above, now will be presented the values of errors calculated between each method used.

$Err_{pre\%,1}$=4.86% and $Err_{post\%,1}$=5.6% represents "pre" and "post" errors between the 50% of points calculated through the mean value between two adjacent columns and the SE calculated in the whole domain (100% of points). The error between the last method and the 50% of points calculated using green and sky-blue elements is $Err_{pre\%,2}$=1.28% and $Err_{post\%,2}$=1.12% while compared to 50% calculated by selecting the white elements there is a $Err_{pre\%,2}$=1.74% and $Err_{post\%,2}$=1.45% respectively for "pre" and "post" sections.

Considering the following notation referred to the method employed:

- method **1** → SE calculated in all the domain, for 100% of the grid elements;
- method **2** → SE calculated for the 50% of the grid elements considering green and sky-blue elements in figure 4.15a;
- method **3** → SE calculated for the 50% of the grid elements considering white elements in figure 4.15a;
- method **4** → SE calculated for the 50% of the grid elements considering the SE average value of two adjacent columns (red dots in figure 4.15b);

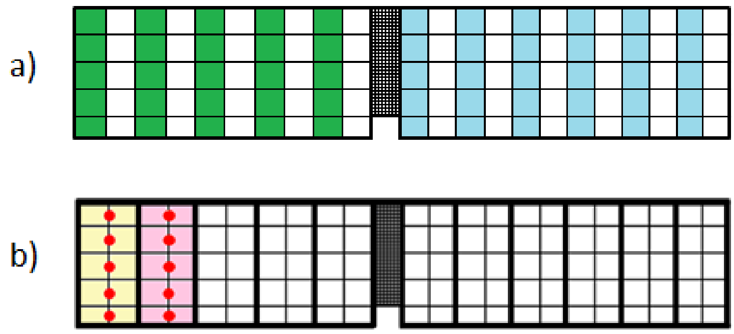

Figure 4.15: Grid elements chosen for the analysis with the 50% of point of SE. a) elements chosen for the first and second method, b) mean value of SE in two adjacent columns.

table 4.1 resume all the SE errors derived by the comparisons mentioned above for a channel with one rectangular obstacle, when it is characterised by a height of $\mathrm{h}_1 = \frac{\mathrm{h}_{\mathrm{ch}}}{6}$ and *Re*=1:

Configuration	Methods	% Error - Pre obstacle	% Error - Post obstacle
1 rectangular at Re=1 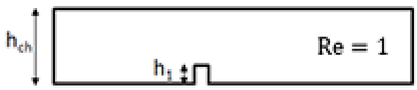	**1 vs 2**	3.93 %	4.6 %
	1 vs 3	3.37 %	4.15 %
	1 vs 4	4.86 %	5.6 %
	2 vs 3	1.03%	0.97 %
	2 vs 4	1.28 %	1.12 %
	3 vs 4	1.74 %	1.45 %

Table 4.1: Results of % error between the different methods used for a channel with one rectangular obstacle at a Re=1.

Since for the other case analysed the values of SE obtained with all methods listed above were much more similar to each other, only the graph with the overlapped SE will be shown.

In order to evaluate the differences, also the semicircular shape for one obstacle at *Re*=1 has been considered.

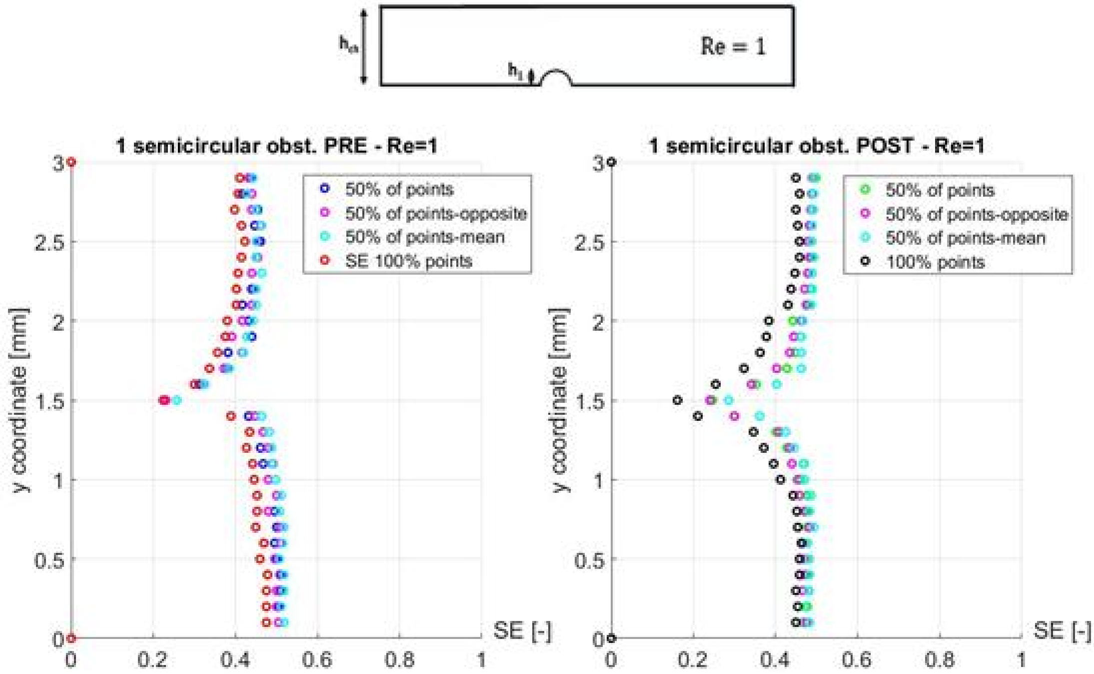

Figure 4.16: Comparison between SE calculated in the whole grid, considering the 50% of points (green and sky-blue), considering the opposite 50% of points (white elements) and averaging between two adjacent columns for one semicircular obstacle in "pre" and "post" section at Re=1.

Also for this configuration is possible to see that there are not great differences between the methods but, however very small, it presents the maximum error in the post obstacle section between the 50% of points calculated through the mean value between two adjacent columns and the SE calculated in the whole domain (100% of points).

Configurations	Methods	% Error - Pre obstacle	% Error - Post obstacle
	1 vs 2	3.22 %	4.48 %
	1 vs 3	3.41 %	3.89 %
1 semicircular at Re=1	**1 vs 4**	4.43 %	5.58 %
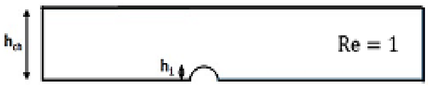	**2 vs 3**	1.08 %	0.93 %
	2 vs 4	1.41 %	1.25 %
	3 vs 4	1.16 %	1.68 %

Table 4.2: Results of % error between the different methods used for a channel with one semicircular obstacle at a Re=1.

Below is presented the result obtained for a channel with two symmetrical and rectangular obstacles at Re = 50 for the sections "pre" and "post" obstacles.

Since considering the SE in the entire channel it provided indications on the symmetry that characterizes this configuration, it was expected that even considering the 50% of the elements of the grid this peculiarity was highlighted.

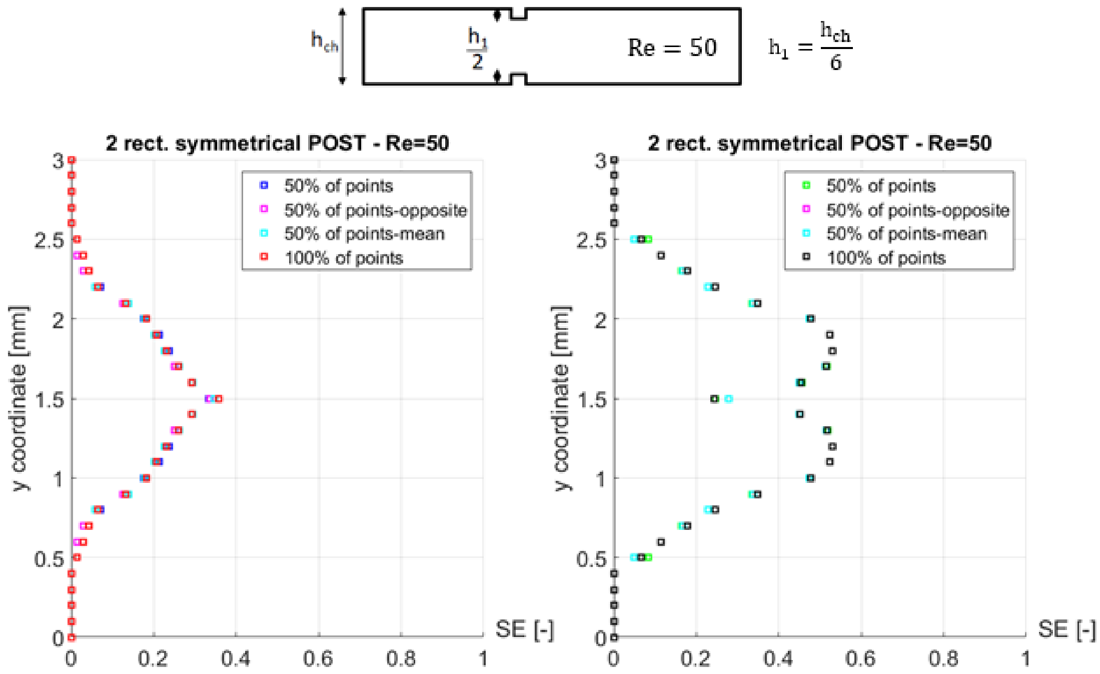

Figure 4.17: A comparison between SE calculated in the whole grid: 1. considering the 50% of points (green and sky-blue); 2. considering the opposite 50% of points (white elements) and 3. averaging between two adjacent columns for two rectangular symmetrical obstacles in “pre” and “post” section at Re=50.

First of all, the results shown that the starting idea about the conservation of symmetry was correct. In this situation, indeed, it can be considered “co-variant” and for each method listed above, the symmetry is maintained.

Numerically, calculating errors through equation 4.2 and 4.3, all the percentage errors are less than 1%. In particular, the maximum error is equal to 0.57% and derived by the SE calculated on 100% of the grid and the SE at 50% of the points calculated as the average of the adjacent cells. The minimum error, on the other hand, is equal to 0.19% and occurs between the last quoted method and the 50% SE considering the white elements of figure 4.15. Table 4.3 resume all the SE errors derived by the comparisons of methods in the configuration explained above, with obstacles characterised by a height of $h_1 = \frac{h_{ch}}{6}$ and at *Re*=50. From this value is possible to see how also the error values reflect the symmetrical geometry because, how seen in figure 4.17, all methods curves are almost coincident and so the errors are very small.

Configuration	Methods	% Error - Pre obstacle	% Error - Post obstacle
	1 vs 2	0.28 %	0.29 %
	1 vs 3	0.48 %	0.38 %
2 symm. Rect. at Re=50	**1 vs 4**	0.25 %	0.56 %
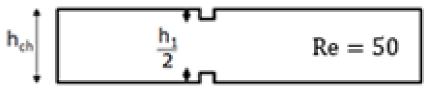	**2 vs 3**	0.57 %	0.37 %
	2 vs 4	0.31 %	0.55 %
	3 vs 4	0.38 %	0.19 %

Table 4.3: Results of % error between the different methods used for a channel with two symmetrical and rectangular obstacle at *Re*=50.

The same case but with the semicircular obstacles was studied. How described in paragraph 4.1 in this situation the obstacles symmetry was not so evident. Compared to the case with a single obstacle, certainly the arrangement of the two obstacles is intuitive, but it is not like as in the rectangular case. Also in this case, therefore, a certain similarity was expected even if the SE was calculated considering 50% of the points. However, at the same time, it was expected that there would be some greater discrepancies whereas not all the elements of the grid appeared in the calculus.

These hypotheses have been confirmed by the graph in figure 4.18. It shows the trend of the SE for all four methods described. A certain difference between the curves is visible, although the shape of the curve is always the same and the values do not differ too much from one another.

About the value of the errors that occur between the different methods, it follows that the maximum error is equal to 4.22% and it corresponds to the difference between the method 1 and 4. The minor error is instead between method 3 and 4 and is equal to 0.7%. Table 4.4 resume all the error values for this configuration.

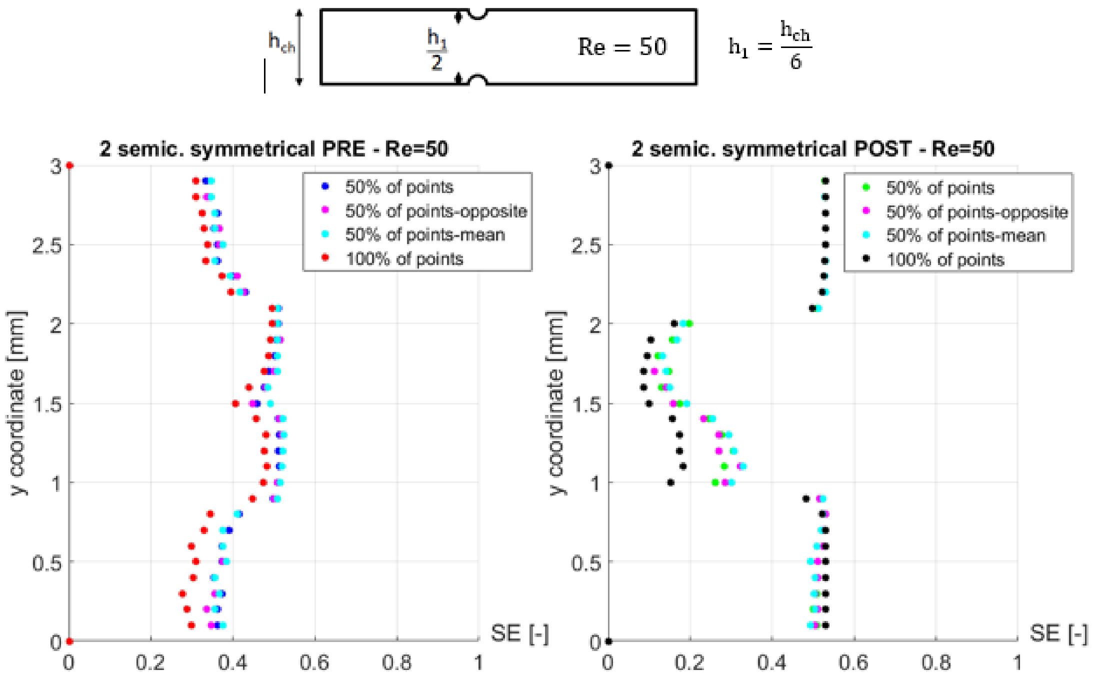

Figure 4.18: Comparison between SE calculated in the whole grid, considering the 50% of points (green and sky-blue), considering the opposite 50% of points (white elements) and averaging between two adjacent columns for two semicircular symmetrical obstacles in "pre" and "post" section at Re=50.

Configuration	Methods	% Error - Pre obstacle	% Error - Post obstacle
	1 vs 2	3.87	3.3
	1 vs 3	3.79	3.2
2 symm. Semi. at Re=50	**1 vs 4**	4.22	4
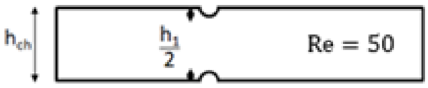	**2 vs 3**	0.74	0.8
	2 vs 4	0.8	0.89
	3 vs 4	0.7	0.83

Table 4.4: Results of % error between the different methods used for a channel with two symmetrical and semicircular obstacle at Re=50.

The last case for which the SE has been evaluated considering only 50% of the points, is the point *c* of figure 4.10: a channel where two obstacles semicircular are alternated. They are in the upper and lower wall but shifted to each other (figure 4.19).

The maximum percentage error is 1.36% and is referred to the difference between the SE in all domain and the SE at 50% including white elements in the "post" obstacles section. Instead, the minimum value is 0.31% and was found between the 4^{th} method (considering the average value between two columns) and the 3^{rd} (white elements in figure 4.15).

Configuration	Methods	% Error - Pre obstacle	% Error - Post obstacle
2 altern. Semi. at Re=50 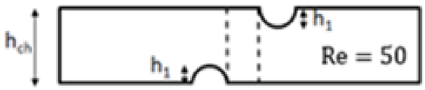	**1 vs 2**	1.21	0.97
	1 vs 3	1.27	1.36
	1 vs 4	1.2	1.14
	2 vs 3	0.56	0.55
	2 vs 4	0.45	0.33
	3 vs 4	0.43	0.31

Table 4.5: Results of % error between the different methods used for a channel with two alternated and semicircular obstacle at Re=50.

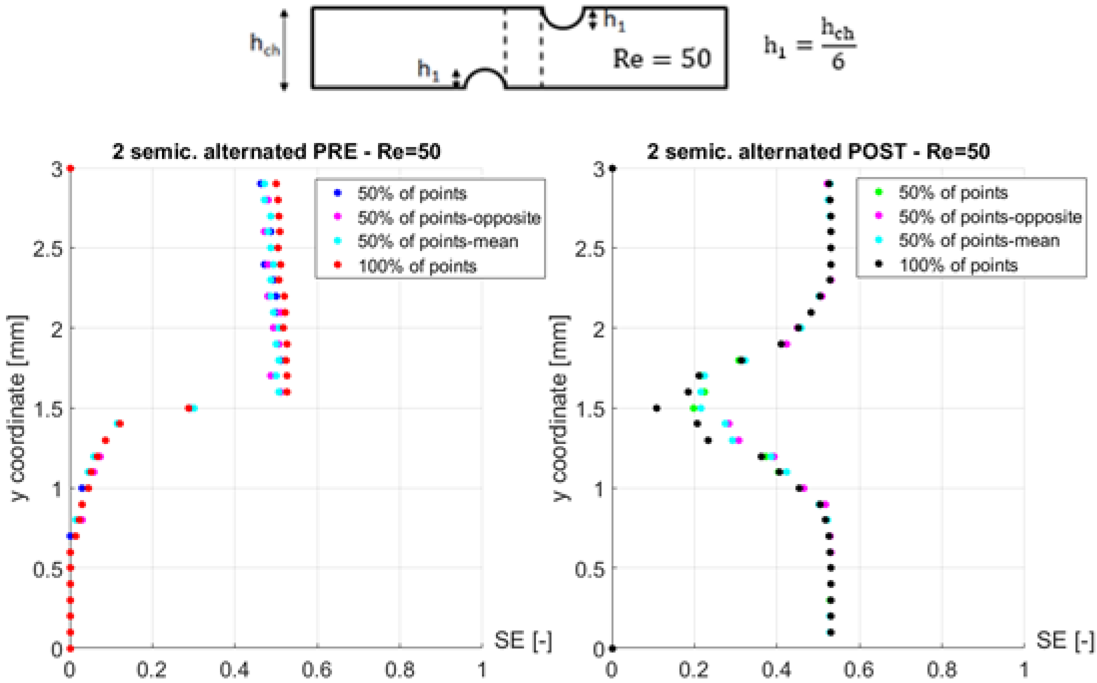

Figure 4.19: Comparison between SE calculated in the whole grid, considering the 50% of points (green and sky-blue), considering the opposite 50% of points (white elements) and averaging between two adjacent columns for two semicircular alternated obstacles in "pre" and "post" section at Re=50.

Considering all the errors values tables, in the following figure are graphed the errors curve with respect to all the obstacles configurations explained above. In the ordinate axis there is the percentage error value. On the abscissas, instead, are indicated the configurations taken into account for this part of the study.

The different curves show the value of the error among the different methods analysed with reference to the notation previously introduced:

- method **1** → SE calculated in all the domain, for 100% of the grid elements;
- method **2** → SE calculated for the 50% of the grid elements considering green and sky-blue elements in figure 15;
- method **3** → SE calculated for the 50% of the grid elements considering white elements in figure 4.15a;
- method **4** → SE calculated for the 50% of the grid elements considering the SE average value of two adjacent columns (red dots in figure 4.15b);

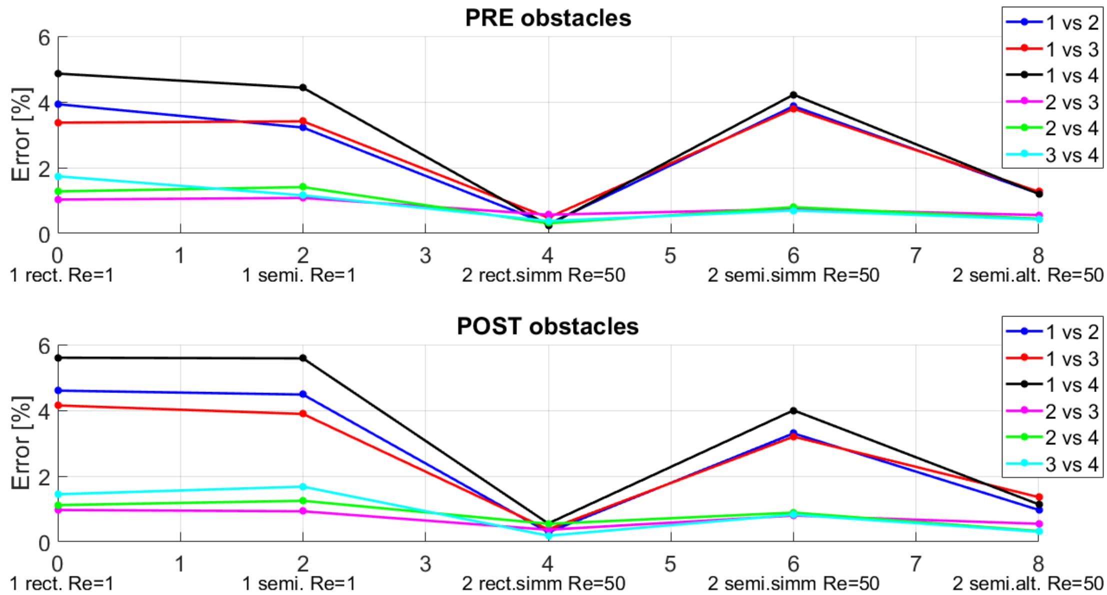

Figure 4.20: errors values between the different methods with respect to the geometrical configuration.

In the graph it is possible to see that in the “pre” and “post” section the trends of the curves are very similar. Furthermore, there is the confirm that in the configuration with two rectangular symmetrical obstacles at *Re*=50 the symmetry of entropy is maintained and it is very strong with all the methods used. It is co-variant: independent of the geometry of points that are analysed. In the other configurations there is an increase of Shannon entropy variation to confirm what had been observed previously. The graphs show a discrepancy based on obstacle configurations. It is always possible to notice a greater error in the case of comparison between the first method (100% of the grid points) with respect to all the other methods (except for the symmetrical case described above), with errors ranging from 4% to 5.6%.

However, keep in mind that there are still very low percentage changes. This therefore assumes that the method is very solid, at least in the analysed 2D cases.

In conclusion, analysing only the half of SE values, has been demonstrated that the SE maintain its trend in all the examinations. The average entropy almost always increases but probably in a not too significant way since, was first established, errors were constantly < 6%.

Chapter 5

Discussion and conclusions

The principal aim of this study was to investigate the behaviour of a fluid that flows in a 2D channel in presence of obstacle/s characterised by different shapes, height, multiplicity and dispositions. This analysis was carried out not mainly by a mechanical point of view, common way to study fluidic systems, but applying an energetical analysis (thermodynamic) focusing on the entropy itself. Moreover, the latter was not studied in a “traditional” way, but employing the Claude Shannon Information Theory, using a different concept of entropy and in order to examine fluid capability to store information.

So, in accord with the method presented before, some interesting considerations about the results obtained and computing simulations done came out.

First of all, this study can be considered as good starting point to suggest the deepening of this analysis to geometrically describe a conduit at the level of presence of obstacles within it. In fact, analysing the parameters linked to entropy, seems to be possible to discriminate their geometry and distribution. The study also highlights what was intuitively mechanical: some configurations regulate the flow and therefore reduce the loss of information compared to standard configurations (i.e. one rectangular and semicircular obstacle).

Through the representation of the Shannon entropy it was possible to notice how this physical concept is able to discriminate the arrangement of the obstacles and their shape thanks to the different types of trends that characterize the different cases.

Realistically, it can be said that the reduction of the points of the domain (and therefore of the sections analysed) does not affect the calculation of the SE. This result is very good because it allows a lower expenditure of resources for the calculation but above all requires less information when checking the values of the SE. It is a result that bodes well for using the SE method in these conditions, for example to reconstruct the geometry of a scaffold in the bioreactor field or for the fluid mixing in the microfluidic field. In this last domain, being able to know the best arrangement of obstacles for the specific case, make possible to create *a priori* a channel that allows for example to have maximum mixing.

The present analysis seems to be sensitive to a range of microfluidic *Re* suggesting therefore its use in this field, but in the next future will be necessary to investigate this important parameter to evaluate the sensitivity of the method. One of the possible applications are certainly microfluidics but also in the field of bioreactors for cells and tissues, therefore for the creation of scaffolds as a culture medium for cell expansion and differentiation.

On the other hand, with the analyses carried out up to now, it is not possible to affirm that the Shannon entropy is able to perfectly describe the internal geometry of a channel in which a fluid flows. But we must remember that it is a preliminary study, one of the first carried out in this sector, and more efforts it required. The question we asked ourselves during the study, found out an answer only partially. From the results obtained, can be deduced that the goal has not been achieved yet but the excellent potential of the method has been.

For the microfluidics field of application, the analysis of the Shannon entropy can be used in two different situations: *a priori* and *a posteriori*.

For the first, supposing to evaluate the degree of mixing between two different substances, and that for the required field of use, the mixing between the two should be maximum. The question that ascends is how to design the channel this result. Parallelism with Shannon entropy arises spontaneously because a maximum mixing results in a very high value of SE (ideally maximum). This situation corresponds to a total loss of information, the system is disordered, that is, the two substances have completely mixed together and it is not possible to distinguish one from the other.

Being able to know the behaviour of Shannon entropy, and therefore the representation of its curves in the presence of obstacles, we could look for a curve that has suitable mixing properties and we could have a feedback on how the obstacles affect the SE. What could be obtained therefore is how to optimize the geometry. Supposing that it is necessary to make a choice about how many obstacles to insert within the channel. For example, 3 obstacles inside instead of 6 could be result more convenient to have. The last situation may have a more stable condition because the fluid does not have enough time to detect the presence of other obstacles and therefore could flow "as if they were not there". So, analysing the SE trends, theoretically, it should be possible to understand what configurations is better for the aim.

In *a posteriori* situation, instead, the Shannon entropy could be used to understand if the mixing between two fluids has happened or not. In fact, if mixing is reached at right conditions, represented by a certain curve, geometrically analysing the conduit through the SE, it would be possible to search if the trend is actually the desired one and if the mixing has been done correctly.

The possibility of investigating the phenomenon within the channel, but only in some points, could be very useful. The idea would be based on the following question: "can the mechanical characteristics provide suggestions on what is happening inside the channel, but not *a priori* (in the design phase) but in *a posteriori* study?".

The Shannon entropy can be also employed for "real time" analysis. Supposing to know how the fluid should behave inside a channel, but observing that this does not actually happen. The idea would be to evaluate what really is happening through precise measurements of the SE, for example with the insertion of a tracer with different viscosity. Evaluating its behaviour at the inlet and outlet of the channel would then be possible to reconstruct the internal geometry of the same.

Also for the bioreactors field mentioned above some possible application can be imagined: to both *a priori* and a *posteriori* analysis. For the former, in the design phase, the SE could be used to define the geometry of a channel (in this case a scaffold) that allows to promote cell growth. Assuming that a channel with rectangular obstacles is more favourable because it has a lower SE, less information loss, and therefore for example less energy dissipation phenomena or turbulent phenomena, certainly in the design phase we would try to reproduce this situation.

An example of a *posteriori* analysis could be the monitoring of the growth cells in a pre-existing scaffold. In fact, knowing the trend of SE in that situation, checking any changes in the progress of the SE, it would be possible to trace a possible change in the internal geometry due to cellular growth/differentiation.

At the end, the method described in the present study, theoretically turns out to be an excellent starting point to actually create a method that allows to discriminate configurations, shapes and multiplicity of obstacles present within a channel. A future prospect is certainly to find a relationship that can make this type of study more applicative. Surely, because the SE has the potential to achieve the goal but not in this range, it is necessary to carry out a study of the study through 3D analysis. In this way it is possible to reconstruct the internal geometry of the channel thanks to a greater number of points starting from methods that refer to the geometrical information (i.e. maximum likelihood).

Surely it is necessary to carry out a more in-depth analysis of the minimum number of points necessary to have discrimination and the determination of the technique with which to operate. It was also important to carry out a farther analysis of the error between the different methods explained in order to understand if it can be relevant for the SE calculus. Even a more detailed evaluation of the suitable *Re* range will surely bring benefits to work. In fact, different Reynolds numbers should be considered, and in particular it would be appropriate to determine if there is a minimum amount of energy to be lost to describe the geometry, as it could happen that from a certain value of Re onwards the loss is so high that detect differences between the different configurations (unreadable).

A step forward through a 3D analysis will be mandatory to verify the goodness of the application of the SE theory here presented. Moreover “fishing” from the statistical mechanics and information geometry will be possible to build out a strong relationship, coupling theory from thermodynamics like SE with the capability of matter to interact with the environment (i.e. fluid in channels).

Bibliography

[1] C. E. Shannon, “A Mathematical Theory of Communication,” *Bell System Technical Journal.,* July–October 1948.

[2] S. Chatti, C. Ghabi and A. Mhimid, “Effect of Obstacle Presence for Heat Transfer in Porous Channel,” in *Design and Modeling of Mechanical Systems - II*, Springer, Cham, 2015, pp. 823-832..

[3] S. Gareh, “Numerical Heat Transfer in a Rectangular Channel with Mounted Obstacle,” *International Letters of Chemistry, Physics and Astronomy,* vol. 38, pp. 111-119, 2014.

[4] K. Bilen and S. Yapici, “Heat transfer from a surface fitted with rectangular blocks at different orientation angle,” in *Heat and mass transfer*, vol. 38, Springer; Verlag, 2002, pp. 649-655.

[5] Y. Wang and K. Vafai, “Heat Transfer and Pressure Loss Characterization in a Channel with Discrete Flush-Mounted and Protruding Heat Sources,” in *Experimental Heat Transfer*, vol. 12, 1999, pp. 1-16.

[6] M. J. Hosseini, M. Farhadi and K. Sedighi, “Effect of wall-mounted obstacles on convective heat transfer in the Poiseulle–Benard channel,” *Facta universitatis, series: mechanical engineering,* vol. 6, pp. 25-36, 2008.

[7] S. J. Cox, “Simulations of bubble division in the flow of a foam past an obstacle in a narrow channel,” *Colloids and Surfaces A: Physicochemical and Engineering Aspects.,* vol. 473, pp. 104-108, 2014.

[8] N. Khasanov, “Acoustic oscillations of a gas near nested thin-walled cylindrical obstacles in a channel,” *J Appl Mech Tech Phy,* vol. 52, pp. 577-584, 2011.

[9] A. Merdasi, S. Ebrahimi, A. Moosavi, M. B. Shafii and F. Kowsaryb, “Simulation of a falling droplet in a vertical channel with rectangular obstacles,” *European Journal of Mechanics - B/Fluids,* vol. 68, pp. 108-117, 2017.

[10] J. Yojina, W. Ngamsaad, N. Nuttavut and e. al., “Investigating flow patterns in a channel with complex obstacles using the lattice Boltzmann method,” *J Mech Sci Technol,* vol. 24, pp. 2025-2034, 2010.

[11] K. Bulusu and M. Plesniak, “Shannon Entropy-Based Wavelet Transform Method for Autonomous Coherent Structure Identification in Fluid Flow Field Data,” *Entropy,* vol. 17, pp. 6617-6642, 2015.

[12] G. Brandani, M. Schor, C. MacPhee, H. Grubmuller, U. Zachariae and e. al., “Quantifying Disorder through Conditional Entropy: An Application to Fluid,” *PLoS ONE 8(6),* 2013.

[13] M. Camesasca, M. Kaufman and I. Manas-Zloczower, “Quantifying fluid mixing with the Shannon entropy,” *Macromol Theor Sim,* vol. 15, p. 595–607, 2006.

[14] J. M. Pozo, A. J. Geers, M. Villa-Uriol and F. A.F., “Flow complexity in open systems: interlacing complexity index based on mutual information,” *J. Fluid Mech.,* vol. 825, pp. 704-742, 2017.

[15] L. B. Rocha, A. L. Randall, N. J. Leite, K. Metze and M. Rossi, “Shannon's entropy and fractal dimension provide an objective account of bone tissue organization during calvarial bone regeneration,” *Microscopy research and technique,* vol. 71, pp. 619-625, 2008.

[16] L. Boltzmann, “Weitere Studien über das Wärmegleichgewicht unter Gasmolekülen,” in *Kinetische Theorie II.*, The Kinetic Theory of Gases. History of Modern Physical Sciences. (2003). pp. 262–349 ed., vol. 67, WTB Wissenschaftliche Taschenbücher, 1872, pp. 275-370.

[17] M. Bal'makov, “Entropy and Disorder,” in *Glass Physics and Chemistry.*, vol. 27, 2001, pp. 287-297..

[18] C. E. Shannon and W. Weaver, A Mathematical Theory of Communication, Champaign, IL, USA.: University of Illinois Press, 1963.

[19] M. Tribus and E. C. McIrving, “Energy and Information,” *Scientific American,* vol. 225, pp. 179-188, 1971.

[20] A. Lesne, “Shannon entropy: A rigorous notion at the crossroads between probability, information theory, dynamical systems and statistical physics,” *Mathematical Structures in Computer Science,* vol. 24, 2014.

[21] R. Balian, “Entropy, a protean concept,” in *Poincaré Seminar 2003, Progress in Mathematical Physics.*, vol. 38, Basel, Birkhäuser Verlag, 2004, pp. 119-144..

[22] L. Brillouin, “The negentropy principle of information,” *Journal of Applied Physics,* vol. 24, pp. 1152-1163, 1953.

[23] N. Wiener, Cybernetics, or control and communication in the animal and the machine, Cambridge (Mass.): The MIT Press, 1948.

[24] Y. Çengel, Introduction to thermodynamics and heat transfer, The McGraw-Hill Companies, S.r.l., 2008.

[25] J. Maxwell, Theory of Heat, Third Edition ed., London: Longmans, Green, and Co., 1872.

[26] F. Boschetto, “fmboschetto,” 28 novembre 2001. [Online]. Available: http://www.fmboschetto.it/tde3/termod7.htm. [Accessed 2018].

[27] L. Szilard, “Über die Entropieverminderung in einem thermodynamischen System bei Eingriffen intelligenter Wesen (On the reduction of entropy in a thermodynamic system by the intervention of intelligent beings),” in *Zeitschrift für Physik*, 1929, pp. 840-856.

[28] R. Landauer, “Irreversibility and heat generation in the computing process,” *IBM Journal of Research and Development.,* 1961.

[29] M. Camesasca, M. Kaufman and I. Manas-Zloczower, “Quantifying fluid mixing with the Shannon entropy,” *Macromol. Theory Simul.,* vol. 15, no. 8, p. 595–607., 2006.

[30] Ç. Y. and J. M. Cimbala, Fluid mechanics: fundamentals and applications, McGraw-Hill Higher Education., 2006.

[31] G. M. Carlomagno, Fluidodinamica, Liguori, 2004.

[32] A. Dumas, Elementi di fluidodinamica e termocinetica, Esculapio, 2003.

[33] G. Batchelor, Introduction to Fluid Mechanics, Cambridge Mathematical Library, 2000.

Appendix A

In chapter 3, in the paragraph "**3.6 Average entropy and centre of distribution**", the method by which the two parameters "centre of distribution" and "average entropy" were calculated has been described. In particular, the average Shannon entropy was calculated as:

$$\text{Average SE} = \frac{\sum_{i=1}^{31} M_i \cdot SE_i}{\sum_{i=1}^{31} M_i}$$

while the centre of distribution as:

$$y' \cdot \left(\sum_{i=1}^{16} SE_i \right) = \left(\sum_{i=16}^{31} SE_i \right) \cdot (3 - y')$$

$$\text{Centre of distribution} = \frac{3 \cdot \sum_{i=16}^{31} SE_i}{\sum_{i=1}^{31} SE_i}$$

where the y axis represents the variations in the height of the channel.

The aim of studying these two parameters was to investigate the distribution of SE in both x and y coordinate in order to characterise spatially the value of SE. The initial idea was to evaluate how they varied with respect to the shape, position, size and multiplicity of obstacles, i.e. if they could be useful parameters for the discrimination of the internal geometry of the channel.

This analysis was carried out for all the configurations and all the heights of the obstacles presented in **table 3.1**. For the final study, however, we focused on other aspects, so these results are not analysed in detail in this work. The graphs obtained for the configurations examined in detail in the previous chapters (**figure 4.1**) are presented below.

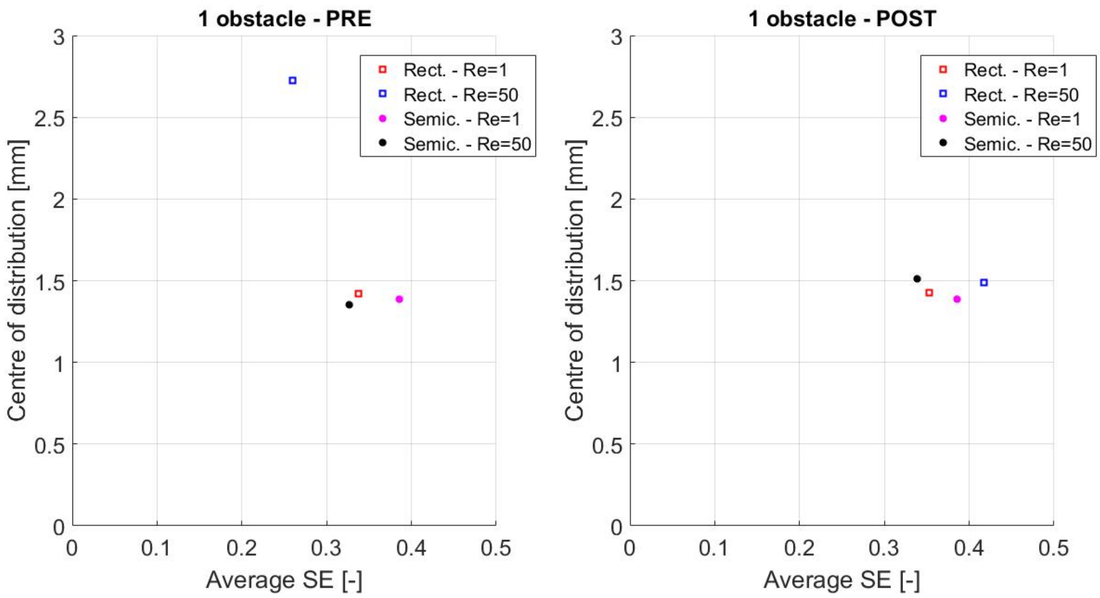

Average SE and centre of distribution for one obstacle, rectangular and semicircular, at Re=1 and Re=50. The figure shown similar values for all cases in pre and post sections, except for the case of rectangular obstacles at Re=50 in according with the SE trend for this configuration.

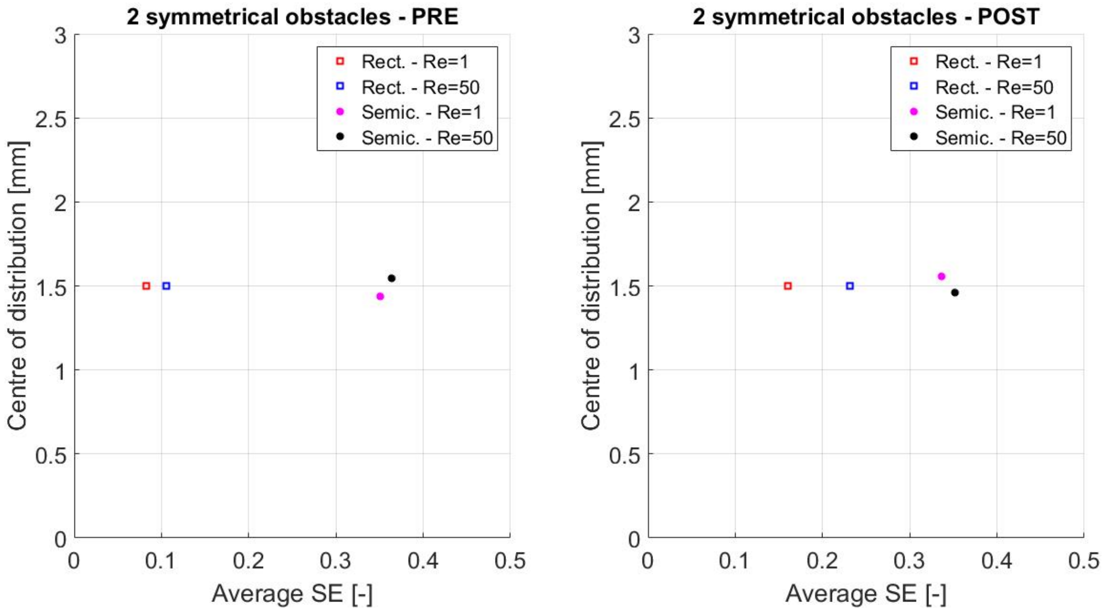

Average SE and centre of distribution for two symmetrical obstacles, rectangular and semicircular, at Re=1 and Re=50. All values underline the symmetry of the obstacles, especially for the rectangular cases. Moreover, the closed values are grouped based on the shape of the obstacle.

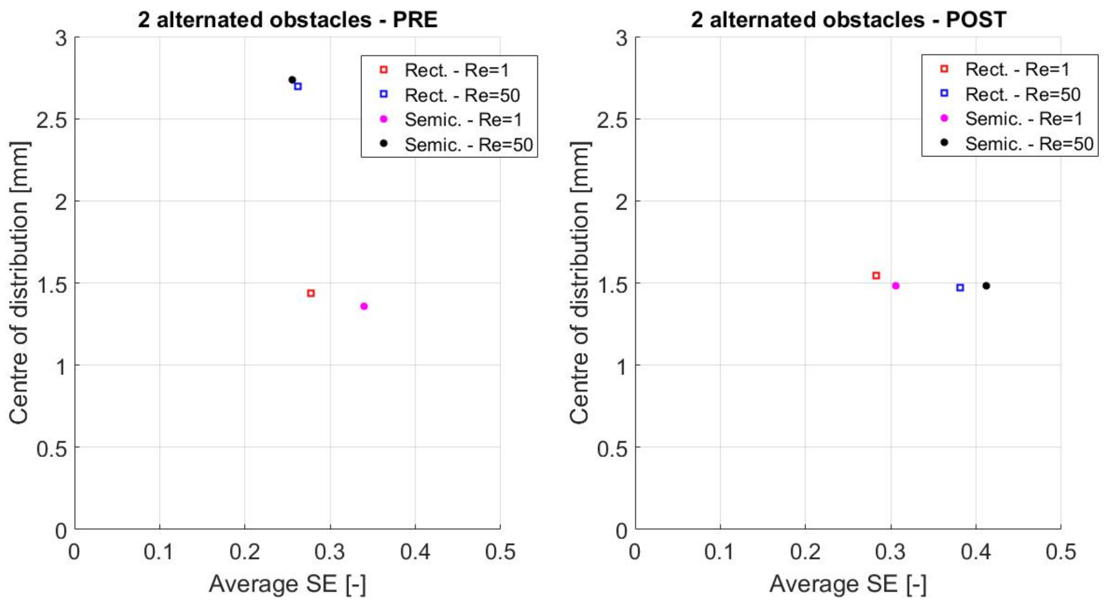

Average SE and centre of distribution for two alternated obstacles, rectangular and semicircular, at Re=1 and Re=50. The closed values are grouped based on the Re values.

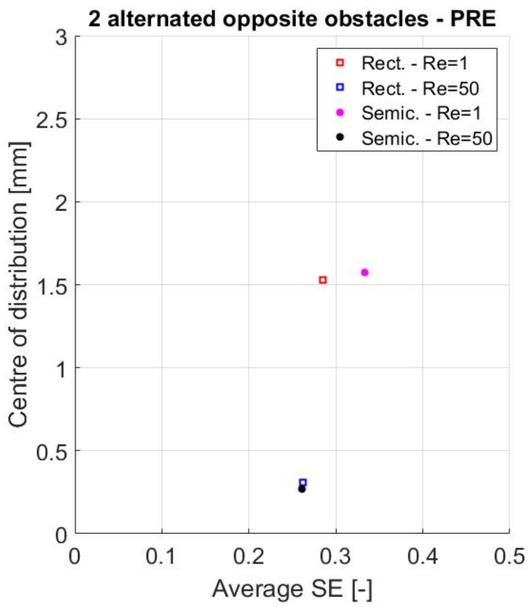

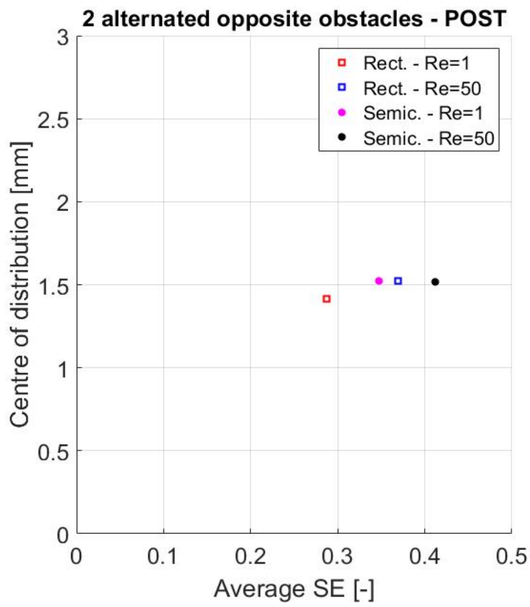

Average SE and centre of distribution for two alternated opposite obstacles, rectangular and semicircular, at Re=1 and Re=50. In the pre section the closed values are grouped based on the Re values. In the post sections instead the values are more similar and, except for the rectangular case at Re=1, they are collocated in the half of the channel.